Report No. CG-D-09-94

EVALUATION OF NIGHT CAPABLE SENSORS FOR THE DETECTION OF OIL ON WATER

G. L. HOVER
U.S. Coast Guard Research and Development Center
1082 Shennecossett Road, Groton, Connecticut 06340-6096

AND

J. V. PLOURDE
Analysis & Technology, Inc.
258 Bank Street, New London, Connecticut 06320

FINAL REPORT

MARCH 1994

Prepared for :

U.S. Department of Transportation
United States Coast Guard
Office of Engineering, Logistics, and Development
Washington, DC 20593-0001

NOTICE

This document is disseminated under the sponsorship of the Department of Transportation in the interest of information exchange. The United States Government assumes no liability for its contents or use thereof.

The United States Government does not endorse products or manufacturers. Trade or manufacturers' names appear herein solely because they are considered essential to the object of this report.

The contents of this report reflect the views of the Coast Guard Research & Development Center. This report does not constitute a standard, specification, or regulation.

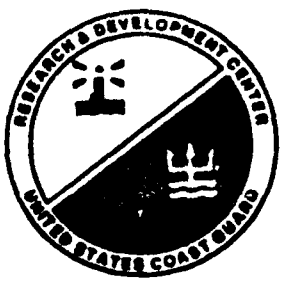

D. L. Motherway
Technical Director, Acting
United States Coast Guard
Research & Development Center
1082 Shennecossett Road
Groton, CT 06340-6096

Technical Report Documentation Page

1. Report No.	2. Government Accession No.	3. Recipient's Catalog No.
CG-D-09-94		

4. Title and Subtitle	5. Report Date
Evaluation of Night Capable Sensors for the Detection of Oil on Water	March 1994
	6. Performing Organization Code
7. Author(s) G.L. Hover and J.V. Plourde	8. Performing Organization Report No. R&DC 09/94

9. Performing Organization Name and Address		10. Work Unit No. (TRAIS)
U.S.C.G. R&D Center 1082 Shennecossett Road Groton, CT 06340-6096	Analysis & Technology, Inc. 258 Bank Street New London, CT 06320	11. Contract or Grant No. N66604-93-D-1119/0033

12. Sponsoring Agency Name and Address	13. Type of Report and Period Covered
Department of Transportation U.S. Coast Guard Office of Marine Environmental Protection Washington, D. C. 20593	Final Report May 1993 - March 1994
	14. Sponsoring Agency Code

15. Supplementary Notes

This report documents the evaluation of several readily-available night imaging devices for detection of oil slicks. This research was conducted as part of the USCG R&D Center's Comprehensive Marine Environmental Protection Project's remote sensing research program.

16. Abstract

During May, 1993, the USCG participated in a field exercise conducted at the Canadian Forces Base, Petawawa, Canada. Environment Canada set up a test facility that consisted of a lined pool separated into twelve individual tanks. Four types of petroleum products were added to nine of the tanks while three tanks were left clean as control tanks. The field exercise provided an opportunity to evaluate several night-capable sensors for detection of oil slicks on water.

The USCG evaluated the day and night imaging capabilities of long wave infrared (LWIR) sensors (FLIR 2000, WF-360TL, and RS-18C) installed on three Coast Guard aircraft. Three commercially-available hand-held medium wave infrared (MWIR) sensors (AGEMA Thermovision 210, FSI PRISM, and IRC-160ST) were also evaluated. Surface truth data were collected at the test site and through the use of visible-spectrum imagers (S-VHS camcorder and WF-360TL TV camera - day and Dark Invader Owl NVG camcorder - night). Sensor imagery was recorded to S-VHS tape format for post exercise review and processing

Analysis of the images confirmed several aspects of expected phenomenology. Both IR and visible spectrum sensors were readily able to detect the oil slicks during daytime sorties. The LWIR (8-12 micron) sensors clearly depicted the oil/water boundary both test nights while the MWIR (3-5 micron) sensors acheived mixed results with marginal oil/water contrast. At night, the NVG camcorder (visible spectrum) provided useful surface truth data but may not provide sufficient image detail when used in an open water environment.

17. Key Words	18. Distribution Statement
Infrared, Infrared Imagers, Long Wave Infrared, Medium Wave Infrared, Night Vision Goggles, Oil Slick Detection, Visible Spectrum, Remote Sensing of Oil Slicks	Document is available to the U.S. Public through the National Technical Information Service, Springfield, VA 22161

19. Security Classif. (of this report)	20. Security Classif. (of this page)	21. No. of Pages	22. Price
UNCLASSIFIED	UNCLASSIFIED		

METRIC CONVERSION FACTORS

Approximate Conversions to Metric Measures

Symbol	When You Know	Multiply By	To Find	Symbol
	LENGTH			
in	inches	*2.5	centimeters	cm
ft	feet	30	centimeters	cm
yd	yards	0.9	meters	m
mi	miles	1.6	kilometers	km
	AREA			
in^2	square inches	6.5	square centimeters	cm^2
ft^2	square feet	0.09	square meters	m^2
yd^2	square yards	0.8	square meters	m^2
mi^2	square miles	2.6	square kilometers	km^2
	acres	0.4	hectares	ha
	MASS (WEIGHT)			
oz	ounces	28	grams	g
lb	pounds	0.45	kilograms	kg
	short tons (2000 lb)	0.9	tonnes	t
	VOLUME			
tsp	teaspoons	5	milliliters	ml
tbsp	tablespoons	15	milliliters	ml
fl oz	fluid ounces	30	milliliters	ml
c	cups	0.24	liters	l
pt	pints	0.47	liters	l
qt	quarts	0.95	liters	l
gal	gallons	3.8	liters	l
ft^3	cubic feet	0.03	cubic meters	m^3
yd^3	cubic yards	0.76	cubic meters	m^3
	TEMPERATURE (EXACT)			
°F	Fahrenheit temperature	5/9 (after subtracting 32)	Celsius temperature	°C

*1 in = 2.54 (exactly)

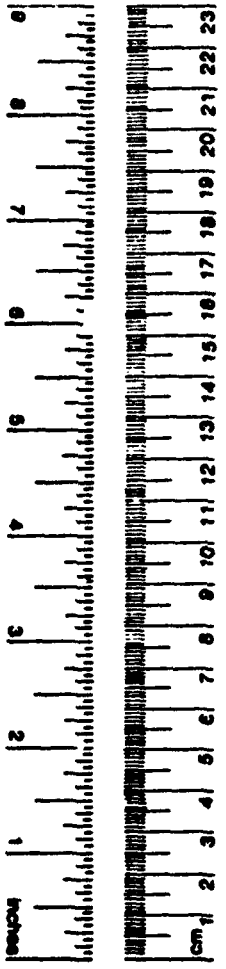

Approximate Conversions from Metric Measures

Symbol	When You Know	Multiply By	To Find	Symbol
	LENGTH			
mm	millimeters	0.04	inches	in
cm	centimeters	0.4	inches	in
m	meters	3.3	feet	ft
m	meters	1.1	yards	yd
km	kilometers	0.6	miles	mi
	AREA			
cm^2	square centimeters	0.16	square inches	in^2
m^2	square meters	1.2	square yards	yd^2
km^2	square kilometers	0.4	square miles	mi^2
ha	hectares (10,000 m^2)	2.5	acres	
	MASS (WEIGHT)			
g	grams	0.035	ounces	oz
kg	kilograms	2.2	pounds	lb
t	tonnes (1000 kg)	1.1	short tons	
	VOLUME			
ml	milliliters	0.03	fluid ounces	fl oz
l	liters	0.125	cups	c
l	liters	2.1	pints	pt
l	liters	1.06	quarts	qt
l	liters	0.26	gallons	gal
m^3	cubic meters	35	cubic feet	ft^3
m^3	cubic meters	1.3	cubic yards	yd^3
	TEMPERATURE (EXACT)			
°C	Celsius temperature	9/5 (then add 32)	Fahrenheit temperature	°F

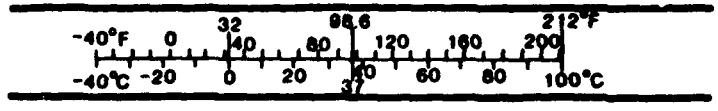

TABLE OF CONTENTS

Section		Page
	LIST OF ILLUSTRATIONS	vi
	LIST OF TABLES	vii
	LIST OF ACRONYMS	viii
	EXECUTIVE SUMMARY	ix
	ACKNOWLEDGMENTS	xvi
1	INTRODUCTION	1-1
1.1	Background	1-1
1.2	Infrared Phenomenology Overview	1-2
1.3	Sensor System Descriptions	1-4
1.3.1	Hand-Held Infrared Devices	1-5
1.3.2	Infrared Devices Installed on Coast Guard Aircraft	1-6
1.3.3	Visible-Spectrum Imagers	1-7
1.4	Experiment Description	1-7
1.4.1	Test Site Description	1-8
1.4.2	Experiment Design and Conduct	1-10
1.5	Range of Environmental Parameters Encountered	1-11
1.6	Image Data Preparation	1-13
1.6.1	Creation of Infrared Video Imagery	1-13
1.6.2	Visible Spectrum Reference Images	1-14
1.7	Image Analysis Overview	1-17
2	IMAGERY OVERVIEW	2-1
2.1	Surface Truth Data	2-1
2.2	Representative Imagery From Hand-held MWIR Sensors	2-8
2.2.1	Daytime MWIR Images	2-8
2.2.2	Nighttime MWIR Images	2-14
2.3	Representative Imagery From Installed LWIR Sensors	2-20
2.3.1	Daytime LWIR Images	2-20
2.3.2	Nighttime LWIR Images	2-24
2.4	Ergonomics	2-27
2.5	Selection of Imagery for Detailed Analysis	2-30
3	IMAGE ANALYSIS	3-1
3.1	Comparison of MWIR and LWIR Sensor Images	3-1
3.2	Investigation of Incidence Angle	3-5
3.3	MWIR Specular Reflection	3-9
3.4	Altitude and Field of View	3-10
3.4.1	MWIR Altitude and Field of View	3-10
3.4.2	LWIR Altitude and Field of View	3-10
3.5	Oil Slick Area and Thickness Estimates	3-12
4	CONCLUSIONS AND RECOMMENDATIONS	4-1
4.1	Conclusions	4-1
4.1.1	Infrared Imaging Performance	4-1
4.1.2	Influence of Operational Parameters	4-2
4.1.3	Ergonomics/Human Factors	4-2
4.2	Recommendations	4-3
	REFERENCES	REF-1

LIST OF ILLUSTRATIONS

Figure		Page
1-1	Petawawa Test Facility	1-8
1-2	Sample Daytime Visible Spectrum Imagery	1-15
1-3	Sample Dark Invader Owl Imagery, Night, 5 May 1993, 300 ft.	1-16
1-4	Investigation of NVG Pixel Intensity	1-18
2-1	Daytime Visible Spectrum Imagery, 4 May 1993	2-4
2-2	Daytime Visible Spectrum Imagery, 5 May 1993	2-5
2-3	Daytime Visible Spectrum Imagery, 6 May 1993	2-6
2-4	Dark Invader Owl Imagery, 4 May 1993	2-7
2-5	Dark Invader Owl Imagery, 5 May 1993	2-7
2-6	Agema 210, Daytime, 4 May 1993, 300 ft.	2-9
2-7	IRC 160ST, Daytime, 4 May 1993, 300 ft.	2-10
2-8	FSI Prism, Daytime, 4 May 1993, 300 ft	2-11
2-9	Agema 210, Daytime, 6 May 1993, 500 ft.	2-12
2-10	IRC 160ST, Daytime, 6 May 1993, 500 ft.	2-13
2-11	Agema 210, Nighttime, 4 May 1993, 1200 ft.	2-16
2-12	IRC 160ST, Nighttime, 4 May 1993, 1200 ft	2-17
2-13	FSI Prism, Nighttime, 4 May 1993, 1200 ft.	2-18
2-14	IRC 160ST, Nighttime, 5 May 1993, 1200 ft	2-19
2-15	FLIR 2000, Daytime, 6 May 1993, 300 ft	2-21
2-16	WF 360TL, Daytime, 6 May, 1993, 500 ft	2-22
2-17	RS-18C, Daytime, 6 May, 1993, 500 ft	2-23
2-18	RS-18C, Nighttime, 5 May, 1993, 1000 ft.	2-24
2-19	FLIR 2000, Nighttime, 5 May, 1993, 1200 ft.	2-25
2-20	WF 350TL, Nighttime, 5 May, 1993, 1000 ft.	2-26
2-21	Agema 210, Day, 6 May 1993, 300 ft.	2-29
3-1	Comparative Imagery, Night, 4 May 1993, 1200'	3-2
3-2	Comparative Imagery, Night, 5 May 1993, 1200'	3-3
3-3	WF-360TL, Day, 5 May 1993, 1000 ft., White Hot Pass	3-6
3-4	WF-360TL, Day, 5 May 1993, 1000 ft., Black Hot Pass	3-7
3-5	WF-360TL, Day, 5 May 1993, 1000 ft., (off nadir view)	3-8
3-6	IRC-160ST Image Showing Specular Reflection	3-9
3-7	IRC-160ST, Black = Hot, Night, 5 May, 1993, Altitude Comparison. (50mm lens)	3-11
3-8	Example of Measuring Oil Slick and Tank Boundaries	3-13

LIST OF TABLES

Table		Page
1	Sensors Evaluated by the USCG	x
1-1	Sensors Evaluated by the USCG	1-5
1-2	*Oil Time and Quantity Release Schedule*	1-9
1-3	Participating Coast Guard Units	1-10
1-4	Range of Atmospheric Parameters Encountered	1-12
1-5	Test Tank Water Temperatures	1-13
2-1	Summary of Altitudes At Which Sensor Imagery Were Obtained	2-3
3-1	Oil Thickness Estimates in Millimeters from 5 May Image and Surface Truth	3-14

LIST OF ACRONYMS

BMP	Bit-mapped
FLIR	Forward Looking Infrared
FOV	Field of View
FSI	FLIR Systems, Inc.
HgCdTe	Mercury Cadmium Telluride
InSb	Indium Antimonide
IR	Infrared
IR/UV	IR/Ultraviolet
km/hr	Kilometers per Hour
kPa	Kilopascal
LWIR	Long-Wave Infrared
MEP	Marine Environmental Protection
mm	Millimeter
MMI	Man-Machine Interface
MOU/JPA	Memorandum of Understanding/Joint Project Agreement
MRTD	Minimum Resolvable Temperature Difference
MWIR	Medium-Wave Infrared
NFOV	Narrow Field of View
NVG	Night Vision Goggle
PbSe	Lead Selenide
PtSi	Platinum Silicide
R&D Center	Research and Development Center
USCG	United States Coast Guard
WFOV	Wide Field of View
℃	Degrees Celsius

EXECUTIVE SUMMARY

INTRODUCTION

1. Background

This report documents a United States Coast Guard (USCG) Research and Development Center (R&D Center) evaluation of several night-capable sensors for the detection of oil on water. This project was performed in support of the USCG marine environmental protection (MEP) program. The primary objective of this project was to evaluate existing, night-capable sensor technologies for their utility in providing a first-response oil spill remote sensing capability to USCG marine pollution control units.

An essential component of this evaluation was the USCG participation, at the invitation of Environment Canada's Emergencies Science Division, in a joint oil spill sensor test conducted from 3 through 7 May 1993 at a test site in Petawawa, Ontario, Canada. During the USCG portion of this experiment, three types of hand-held infrared (IR) devices, two types of installed forward looking infrared (FLIR) devices, a night vision capable video camera, an IR/ultraviolet (IR/UV) line scanner, and an S-VHS video camera were used to image the oil. USCG HH-60J, HU-25B, and HU-25C aircraft participated in the evaluation.

Data from this evaluation will be used to:

1. Compare the performance of three hand-held IR devices operating in the medium-wave infrared (MWIR) band (3 to 5 micrometer (μ) wavelengths);

2. Compare the performance of three aircraft-mounted IR devices operating in the long-wave infrared (LWIR) band (8 to 14μ wavelengths);

3. Compare the relative detection performance of MWIR and LWIR devices against oil-on-water targets;

4. Compare the images produced by the IR devices to daytime video camera and nighttime night vision camera images;

5. Illustrate the effects of operational factors (such as angle of incidence, sensor altitude, and video polarity) and environmental factors (such as differential heating, solar reflections, and oil emulsification) on infrared image quality;

6. Estimate oil thickness from observed slick surface areas and known oil quantities; and

7. Develop recommendations for future evaluation work.

This report provides a primarily-qualitative analysis and interpretation of the imagery obtained during the sensor test. A companion report applies the fundamental theory (based on physical processes) of oil/water contrast signatures to analyze the image data. The companion report predicts contrast signatures that are consistent with the qualitative observations made here.

2. Sensor Descriptions

Table 1 provides a brief description of the sensors, their mode of operation and the frequency range in which they operate. The hand-held units and FLIR 2000 were operated from an HH-60J helicopter, the WF-360TL was operated from the HU-25C, and the RS-18C was operated from the HU-25B.

Table 1. Sensors Evaluated by the USCG

SENSOR	MODE OF OPERATION	INFRARED BAND (μ)
AGEMA 210	Hand-Held IR Camera	3 to 5
IRC-160ST	Hand-Held IR Camera	3 to 5
FSI PRISM	Hand-Held IR Camera	3 to 5
FLIR 2000	Installed IR System	8 to 12
WF-360TL (IR)	Installed IR/Video System	8 to 12
RS-18C	IR/UV Line Scanner	8 to 14
DARK INVADER OWL	Night Vision Camcorder	0.6 to 0.9
HAND-HELD S-VHS	S-VHS Camcorder (color)	visible
WF-360TL (Video)	CCD Video camera (b&w)	visible

3. Experiment Description

The experiment was conducted from 4 to 7 May, 1993 at a specially prepared test site on the Canadian Forces Base Petawawa, Ontario, Canada. Environment Canada created the test facility specifically for this experiment. They administered all aspects of oil release and measurement, recorded environmental conditions during all flights, and scheduled time windows to be used by each of the participating agencies.

The test site consisted of a tank 100 feet wide by 480 feet long, that was built at a remote location on the Petawawa military base. The tank was subdivided into 12 plastic-lined tanks bounded by mounds of soil. Nine of the 12 tanks contained an oil-on-water slick. The remaining three tanks were filled with water as control targets. Figure 1-1 depicts the test bed. From west to east, tanks 4, 8, and 11 were control tanks with no oil added; tanks 1, 2, 3, and 5 were re-oiled each day; and tanks 6, 7, 9, 10, and 12 were oiled on 4 May 1993 and allowed to weather.

Three types of Coast Guard aircraft participated. An HH-60J flew data recording passes at 300, 500, and 1200 feet, an HU-25C and an HU-25B flew data recording passes at 500, 1000, and 1500 feet. Each sensor was operated in white = hot and black = hot video polarities and in wide and narrow field of view where available.

Data imagery was recorded on S-VHS tape for post experiment analysis. A video capture board was used to digitize video frames and permit manipulation for image analyses. The images were stored as 8-bit gray-scale images.

RESULTS

1. Infrared Imaging Performance

Daytime Oil/Water Contrast

All sensors tested provided the ability to reliably detect oil slicks during daytime sorties in a variety of weather. The daytime temperature differences between oil and water provided better information about the relative oil thickness and area coverage than was possible with the visible spectrum images. Under sunny conditions, specular reflection of solar MWIR energy from the water's surface can interfere with the ability to view scene details.

Nighttime Oil/Water Contrast

Nighttime imaging of the test tanks is where the LWIR FLIR imagers proved most advantageous over the other sensors. During the nighttime sorties, the oil and water were estimated to be at the same physical temperature. Under these conditions, the MWIR sensors achieved mixed results and appeared to be sensitive to small changes in environmental conditions and sensor tuning. The LWIR sensors benefited from a significantly higher contrast excess and successfully imaged all test tank oil slicks during two night sorties.

MWIR Image Acuity

The IRC-160ST images, when properly tuned, were very clear. With an intermediate-resolution focal plane array, the IRC-160ST displayed a tendency to create a stepped look to linear features when the imager was tilted diagonally with respect to those features. The magnitude of this distortion was minor and did not detract significantly from image interpretability. The FSI Prism provided high spatial resolution in the images; however, system noise caused the images to have the appearance of being taken through frosted glass. The lower pixel resolution of the Agema 210 (which is significantly cheaper and smaller than the other two hand-held sensors) resulted in blocky images that lacked fine spatial detail.

LWIR Image Acuity

The FLIR 2000 and WF-360TL provided the ability to observe fine detail in the slicks where sufficient oil/water contrast existed. The narrow field of view modes of both LWIR FLIRs provided excellent oil slick spatial detail at altitudes from 300 to 1500 feet. Altitudes of 1200 to 1500 feet reduced the test tank to a size such that the oil slicks were detected but lacking spatial detail when the FLIRs were operated in wide field of view. The scale of the images provided by the RS-18C was too large to be useful in this evaluation. Even at 500 feet, which is typically the lowest practical altitude for searches with this sensor, image detail in the small test tank area was insufficient for a fair comparison to the FLIR sensors.

2. Influence of Operational Parameters

Incidence Angle

Incidence angle appears to affect FLIR ability to depict oil/water contrast only in marginal contrast situations. This result implies that wide-area IR scanning of oil slicks at low incidence should be successful under most conditions (steep depression angles are not essential to oil slick detection).

Video Polarity

Both white = hot and black = hot video polarities were able to provide detailed images. Video polarity can be used to brighten or darken an overall scene. It alters the perception of the scene, but does not provide finer detail or contrast capabilities.

Altitude/Field of View

Altitude affects the field of view and image detail. In general, increased altitude permits viewing more scene with less available detail. At altitudes above 1000 feet, wide field of view images depicted the oil/water contrast at oil slick boundaries; however, observation of slick edge details and/or contrast variations within the oil slicks required lower altitudes, or in the case of the WF-360TL and FLIR 2000, narrow field of view selection.

3. Ergonomics/Human Factors

Hand-held Sensor Design

Throughout the experiment, operators of the hand-held units experienced trouble with overly-sensitive tuning and focus controls. Often, when an operator first used a sensor, the image quality was sometimes unusable. Even after operators became more familiar with the sensors controls a slip of the finger could drastically reduce image quality.

Another difficulty encountered during the test was keeping track of the MWIR imagers, power supplies, and cables, along with their associated recording/display system, while operating in a helicopter environment.

Operator Training

The hand held units (MWIR sensors) were unfamiliar to the operators, and on each successive day of use, the ability of the sensor operators to properly tune the test tank image improved. Night searches during this field test provided ample demonstration of how a lack of sensor familiarity can hinder image collection. When using the hand-held sensors, inexperienced operators often lowered the instruments to their laps to locate desired adjustment controls and then had to relocate the test tanks while attempting to tune the image. Quite often, when an inadvertent change in sensor settings occurred while the sensor was away from the operator's eye, a significant amount of time was spent re-acquiring the image.

CONCLUSIONS

1. Either MWIR or LWIR sensors can reliably image oil slicks on water during the day. The contrast excess available with the LWIR sensors indicates that these are a better choice for night use.

2. Where sufficient IR contrast exists between oil and water, the IRC-160ST and FLIR PRISM MWIR imagers and both LWIR FLIRs provide good spatial resolution and image quality for oil slick identification and tracking.

3. Both daytime and nighttime visible spectrum imagery provided a useful complement to IR imagery for finding oil slick boundaries.

4. The IR imagers are capable of effective oil slick surveillance over a wide range of incidence angles. In marginal contrast situations, changing the incidence angle may improve oil slick visibility.

5. Both the white = hot and the black = hot video polarity provided similar contrast, clear image detail, and equivalent resolution.

6. As expected, altitude significantly affects image content and quality. A lower altitude provides greater scene detail; however, it also limits the field of view. While this is true for both fixed lens and switchable lens sensors, the ability to switch from a wide field of view to a narrow field of view permits easier classification of contrast features than does a fixed lens sensor.

7. The large size of the RS-18C FOV did not permit a fair evaluation of its ability to detect and map oil signatures in a test area as small as the Petawawa site.

8. The man-machine interfaces of the fully-integrated FLIR 2000 and WF-360TL FLIRs were easier to operate than those of the hand-held imagers. With the exception of overly-sensitive tuning adjustment controls; however, the unwieldy nature of hand-held sensor operations did not prevent operators from effectively imaging the oil slicks.

RECOMMENDATIONS

1. Operational guidance should be developed for using available IR devices in typical MEP mission areas such as:

- oil or chemical spill quick response,
- MARPOL, and
- marine inspections.

This should be achieved by obtaining IR oil slick images at night, under a broad range of representative operating conditions, with a variety of oil types.

2. When both LWIR and MWIR sensors are available for night oil spill surveillance, LWIR is preferred if a worst-case scenario of oil and water at equal temperature can be expected.

3. The superior nighttime oil/water contrast observed in the LWIR spectral band and the desire for a portable IR sensor indicates that an evaluation of hand-held LWIR sensors should be conducted.

4. When conducting area surveillance of oil slicks, IR sensors should be used in wide field of view at altitudes of 1000 to 1500 feet. Examination of slick edge detail should be done at lower altitudes when using fixed-lens IR sensors or in narrow field of view where available.

5. Simplifying cabling, consolidating components, and providing an automated coarse contrast/tune function to quickly adjust for ambient conditions could reduce the level of distraction to the operator while improving safety and mission effectiveness. Environmental response personnel who are trained to use hand-held sensors during operational missions should be properly fitted with a personal helmet and familiarized with aircraft communications gear and procedures.

6. More detailed analysis should be conducted on the ability of night vision cameras to detect oil slicks in the marine environment. Particular areas of interest include:

- the level of ambient lighting required to detect a slick;
- the ability of aircraft-mounted illuminators to expand the window of NVG use, and
- the ability of this type sensor to provide slick edge details and areal extent.

7. If the effort recommended above is successful, the complementary nature of the daytime WF-360TL IR and television camera images indicates that the addition of a night vision camera capability to FLIR-equipped aircraft may prove to be a valuable aid to nighttime oil slick surveillance.

ACKNOWLEDGMENTS

This sensor evaluation would not have been possible without the invitation extended by Environment Canada to the U.S. Coast Guard for participation in the Petawawa Oil Spill Sensor Test. Heartfelt thanks are extended to Mr. Merv Fingas and Dr. Carl Brown of Environment Canada's Emergencies Science Division for this research opportunity and for their excellent support throughout the planning, execution, and analysis phases of the work.

The support of U.S. Coast Guard Air Stations Cape Cod, Miami, and Traverse City in providing aircraft and crews for the data collection effort was a key factor to project success. Mr. Blaine Bateman, Dr. Robert Hiltabrand, CWO4 Steve Kibner, and Ms. Debra Schofield of the USCG R&D Center provided needed technical support to various phases of this project. CWO4 Robert Melia of USCG Marine Safety Office New Orleans provided essential operational perspectives to the data collection and analysis efforts.

Mr. Gerry Daniels of MIT Lincoln Laboratory applied a high level of expertise in infrared phenomenology and image interpretation to the data analysis work and provided valuable suggestions for improving this document.

Finally, the support of Cincinnati Electronics Corp., FLIR Systems, Inc., and Nite Optics, Inc. in providing the hand-held imagers for evaluation is gratefully acknowledged.

CHAPTER 1
INTRODUCTION

1.1 BACKGROUND

This report documents a United States Coast Guard (USCG) Research and Development Center (R&D Center) evaluation of several night-capable sensors for the detection of oil on water. This project was performed in support of the USCG marine environmental protection (MEP) program. The primary objective of this project was to evaluate existing, night-capable sensor technologies for their utility in providing a first-response oil spill remote sensing capability to USCG marine pollution control units.

An essential component of this evaluation was the USCG participation, at the invitation of Environment Canada's Emergencies Science Division, in a joint oil spill sensor test conducted from 3 through 7 May 1993 at a test site in Petawawa, Ontario, Canada. During the USCG portion of this experiment, three types of hand-held IR devices, two types of installed FLIR devices, a night vision capable video camera, an IR/ultraviolet (IR/UV) line scanner, and an S-VHS video camera were used to image the oil. USCG *HH-60J*, *HU-25B*, and HU-25C aircraft participated in the evaluation.

Data from this evaluation will be used to:

1. Compare the performance of three hand-held infrared (IR) devices operating in the medium-wave infrared (MWIR) band (3 to 5 micrometer (μ) wavelengths);

2. Compare the performance of three aircraft-mounted IR devices operating in the long-wave infrared (LWIR) band (8 to 14μ wavelengths);

3. Compare the relative detection performance of MWIR and LWIR devices against oil-on-water targets;

4. Compare the images produced by the IR devices to daytime video camera and nighttime night vision camera images;

5. Illustrate the effects of operational factors (such as angle of incidence, sensor altitude, and video polarity) and environmental factors (such as differential heating, solar reflections, and oil emulsification) on infrared image quality;

6. Estimate oil thickness from observed slick surface areas and known oil quantities; and

7. Develop recommendations for future evaluation work.

1.2 INFRARED PHENOMENOLOGY OVERVIEW

An object can be detected by a sensor if the difference, or contrast, in radiation reaching the sensor from the object and its immediate vicinity (background) is sufficient. The radiation from the object and its background can be reflected radiation originating from some other source or radiation emitted from the object or background itself. Contrast can be sensed as a relative difference in object and background intensity levels. Relative contrast (reference 1) is defined as:

$$C_R = \frac{J_O - J_B}{J_B} * 100$$

Where,

C_R is the relative contrast expressed as a percentage (usually 0 to 100),

J_O is the energy radiating from the object, and

J_B is the energy radiating from the background.

A given imaging sensor will be characterized as having a minimum detectable contrast, C_0, in appropriate units. An object or feature can be detected with such a sensor if the contrast between the object and its background, C, is greater than this sensor C_0. The eye, under most illumination conditions, senses relative contrast and its relative contrast sensitivity varies from 2 percent during the day to 10 percent or more at night.

During the day oil spills have sufficient contrast with water such that they are usually easily detected by eye. Other means of observation provide very limited additional information about the oil. At night, however, low illumination levels do not provide sufficient reflective energy to make the contrast between oil and water visible to unaided detection. Even the use of sensitive night vision sensors cannot guarantee detection of such weak contrast levels. Nighttime is where other forms of remote sensing, specifically infrared imaging sensors, offer a potential advantage for oil spill detection and characterization..

While reflected radiation (from the sun or other light sources) dominates the visible spectrum, naturally-emitted radiation dominates in the infrared. The predominant natural source of radiation emitted by bodies on the earth's surface is thermal radiation with wavelengths of 3μ and longer. Therefore, sensors operating in the infrared wavelengths, provided they possess the sensitivity to detect the emitted thermal energy contrast, can provide nighttime images where visible spectrum imagers may not.

Remote sensing at thermal-IR wavelengths is usually confined to spectral regions, called atmospheric windows, where the atmosphere is sufficiently transparent to allow radiation to travel over significant path lengths with little absorption. These windows exist principally in the 3.1 to 4.1μ and 4.5 to 5.5μ wavelength bands (MWIR), and the 8 to 12μ wavelength band (LWIR). LWIR sensors are made that extend out to 14μ ; however, there is a steep drop-off in atmospheric transmission from 12 to 14μ and most LWIR sensors do not include this region. Strong absorption bands, resulting principally from atmospheric water vapor and carbon dioxide, effectively eliminate thermal remote sensing outside these regions.

As with visible spectrum energy, the ability of an infrared sensor to detect a thermal contrast boundary depends on the sensitivity of the sensor in its associated spectral band and the percent contrast available at the sensor in that spectral band. While the sensitivity of the sensor is typically fixed for a given ambient scene temperature, the percent contrast available at the sensor depends on many more variables. These include but are not limited to atmospheric conditions such as relative humidity, the relative temperatures of the object and the background (assumed equal for oil on water at night), the relative emissivities of the object and the background, the path length, and the incidence angle. Season and regional location may also affect thermal contrast; however, related factors (such as temperature and humidity) tend to cancel each other so that the overall effect is that performance remains fairly uniform.

The sensors evaluated during the Petawawa test included those operating in both IR spectral bands. The hand held units were all MWIR devices while the aircraft-mounted units were all LWIR devices. The relative performance of these sensors in detecting oil-on-water targets can be expected to vary somewhat with environmental conditions, oil type, and observational geometry. MWIR and LWIR detection performance differ primarily due to the differences in the emissivity of thermal radiation from oil and water in the two wavelength bands. While some attributes of the emissive nature of fluids are constant, other attributes depend on the particular spectral band in which the attribute is being observed. These attributes include the following (reference 2):

- Emissivities for most oils are generally lower than the emissivity of water.
- This difference is emissivity is more pronounced in the LWIR spectral band than in the MWIR spectral band.

During daylight hours solar differential heating causes darker oils to absorb and re-emit more thermal energy than lighter colored oils or clean water. This causes the dark oils to appear as a hotter signal to the IR devices until the heat source (sun) is removed. At night, when the source of differential heating is removed, oils cool to the same temperature as the surrounding water. When this occurs, the relatively small differences in their emissivities become the major source of thermal contrast and the oil slicks' IR signatures weaken, with MWIR contrast expected to diminish more than LWIR contrast.

The fact that less oil/water contrast exists at MWIR wavelengths than at LWIR wavelengths means that, with MWIR imagers, minor changes in sensor settings or environmental conditions are much more likely to determine whether a particular oil slick is detectable. LWIR sensors benefit from a greater signal excess when oil and water are at the same physical temperature, and are likely to provide images with better oil/water contrast.

This report provides a primarily-qualitative analysis and interpretation of the imagery obtained during the sensor test. A companion report (reference 3) applies the fundamental theory (based on physical processes) of oil/water contrast signatures to analyze the image data. The companion report predicts contrast signatures that are consistent with the qualitative observations made here.

1.3 SENSOR SYSTEM DESCRIPTIONS

The USCG R&D Center obtained three hand-held IR imagers for data collection during the joint sensor test in Petawawa. These devices were configured such that their video output was recorded on an S-VHS recorder. In addition, IR and IR/UV devices currently installed onboard CG aircraft were configured to record video output in VHS or S-VHS format. To provide a visual-spectrum reference, an S-VHS camcorder and a night vision-adapted 8-mm video camera (the Dark Invader Owl) were used to provide a video record of target appearance from the same altitudes, aspect angles, and time frames as the IR devices. The imaging devices used during the Petawawa test are listed in table 1-1. More complete system descriptions are provided in sections 1.3.2 through 1.3.4.

Table 1-1. Sensors Evaluated by the USCG

SENSOR	CATEGORY	INFRARED BAND (μ)
AGEMA 210	Hand-Held IR Camera	3 to 5
IRC-160ST	Hand-Held IR Camera	3 to 5
FSI PRISM	Hand-Held IR Camera	3 to 5
FLIR 2000	Installed IR System	8 to 12
WF-360 TL (IR)	Installed IR/Video System	8 to 12
RS-18C	IR/UV Line Scanner	8 to 14
DARK INVADER OWL	Night Vision Camcorder	0.6 to 0.9
HAND-HELD S-VHS	S-VHS Camcorder (color)	visible
WF-360 TL (Video)	CCD Video camera (b&w)	visible

1.3.1 Hand-Held Infrared Devices

Three hand-held IR sensors were tested in this evaluation. These were the AGEMA 210, the IRC-160ST, and the FLIR Systems, Inc. (FSI) Prism. All three of these sensors operated in the MWIR band, were powered by a portable battery pack, and incorporated a self-contained cooler for the detector array. Thermal sensitivities are quoted directly from the manufacturers published product data.

- The AGEMA Thermovision 210, made by Agema Infrared Systems, uses a 48-element Lead Selenide (PbSe) scanning detector array providing an 8- by 16-degree field of view (FOV). The advertised thermal sensitivity is 0.1°C at 30°C.

- The IRC-160ST, made by Cincinnati Electronics Corp., uses a 160- by 120-element Indium Antimonide (InSb) focal plane array, which provides a 9.1- by 6.8-degree FOV with a 50 millimeter (mm) lens. The display incorporates a gray scale tuning status bar to assist the operator with contrast and brightness adjustments. A false color display mode was available but was not tested. The advertised thermal sensitivity is 0.04°K at 300°K noise-equivalent temperature difference.

- The FSI PRISM is made by FLIR Systems, Inc. and uses a 244- by 320-element Platinum Silicide (PtSi) focal plane array providing an 8.5- by 6.5-degree FOV with a 50 mm lens. The advertised thermal sensitivity is 0.1°C at 30°C minimum discernible temperature.

1.3.2 Infrared Devices Installed on Coast Guard Aircraft

Three IR systems which are currently installed onboard Coast Guard aircraft were tested in this evaluation. These were the FLIR Systems, Inc. model 2000 installed on an HH-60J helicopter, the WF-360TL FLIR/TV installed on an HU-25C jet, and the RS-18C line scanner which is part of the HU-25B AIREYE sensor suite. Each of these systems operates in the LWIR band and is part of the standard electronics package onboard the associated aircraft. Thermal sensitivities are quoted from available published system data.

- The FLIR 2000 uses an eight-element Mercury Cadmium Telluride (HgCdTe) scanning detector array (350- by 343-pixels) to provide a wide field of view (WFOV) of 28- by 15-degrees and a narrow field of view (NFOV) of 7 by 3.25 degrees. The advertised WFOV thermal sensitivity is 0.16°C minimum resolvable temperature difference (MRTD) at 0.36 cycles/mrad spatial frequency. Advertised NFOV thermal resolution is 0.18°C MRTD at 1.3 cycles/mrad spatial frequency.

- The WF-360TL includes a Westinghouse FLIR that is mounted with a bore sighted, black-and-white video camera in a gimbaled turret. The FLIR uses a 120-element, HgCdTe scanning detector array to provide a WFOV of 11.1 by 14.8 degrees and a NFOV of 2.7 by 3.6 degrees. The advertised thermal sensitivity is less than 0.11°C noise-equivalent temperature difference and less than 0.33°C minimum resolvable temperature difference. Spatial frequency was not specified for these advertised thermal sensitivities.

- The RS-18C IR/UV line scanner is a pod-mounted component of the Coast Guard's multi-sensor AIREYE package. The IR component of the sensor consists of a 2-element HgCdTe detector. A rotating mirror scans ±50 degrees perpendicular to the aircraft track to provide a 100-degree FOV centered directly beneath the aircraft. Thermal resolution is 0.2°C noise-equivalent temperature difference on the IRLO channel and 0.02°C noise-equivalent temperature difference on the IRHI channel. Spatial resolution is 2.5 mrad (along-track) by 2.5 mrad (cross-track) on IRLO and 18 by 2.5 mrad on IRHI.

1.3.3 Visible-Spectrum Imagers

Three forms of visible spectrum ground truth imagery were obtained. These were from an S-VHS camcorder, the WF-360TL gimbal mounted TV camera, and the Dark Invader Owl recording to 8-mm video tape.

The hand-held S-VHS camcorder is an off-the-shelf unit with integral battery. The Dark Invader Owl integrates an off-the-shelf High-8 minicam, a Gen III night vision goggle (NVG) image intensifier tube, a 50 mW focusable laser illuminator, and interchangeable lenses (50 mm, 75 mm, and 75-300 mm zoom). S-VHS (daytime) and Dark Invader Owl (nighttime) imagery were recorded from the HH-60J door on a not-to-interfere basis during IR imaging from the hand-held IR sensors.

The WF-360TL incorporated a black-and-white CCD video camera in the gimbal mount. During the day, this camera was a particularly useful surface-truth sensor because it was bore sighted with the WF-360TL FLIR imager, providing simultaneous visible spectrum and infrared images.

1.4 EXPERIMENT DESCRIPTION

The experiment was conducted from 4 to 7 May, 1993 at a specially-prepared test site on the Canadian Forces Base Petawawa, Ontario, Canada. The Emergencies Science Division of Environment Canada planned the test to evaluate the ability of prototype airborne laser-acoustic and laser fluorosensor devices to detect, identify, and quantify oil slicks. Under an existing Memorandum of Understanding/Joint Project Agreement (MOU/JPA) between the USCG R&D Center and the Emergencies Science Division of Environment Canada (promoting cooperation in testing and development of oil spill sensors) the R&D Center was invited to use the test site to evaluate sensors of interest to the USCG. Environment Canada created the test facility specifically for this experiment, administered all aspects of oil release and measurement, recorded environmental conditions during all flights, and provided time windows to be used by each of the participating agencies.

1.4.1 Test Site Description

A test tank 100 feet wide by 480 feet long was built at a remote location on the Petawawa military base. The tank was subdivided into 12 plastic-lined tanks bounded by mounds of soil. Nine of the 12 tanks contained oil-on-water slicks. These were subdivided with a center berm (thus creating 18 oiled cells) to baffle the effects of wind on the oil in an attempt to ensure that there was always some oil near the center of the tank, regardless of wind direction. The remaining three tanks were filled with water as control targets. Figure 1-1 depicts the test bed.

Each of the 12 tanks were filled with fresh lake water to a depth of 6 inches. Two tanks (11 and 12) were salted (3.3% sodium chloride) to simulate ocean water. Four types of oil products were released in the nine baffled tanks according to the schedule provided in table 1-2. As shown in table 1-2, tanks 4, 8, and 11 were control tanks with no oil added; tanks 1, 2, 3, and 5 were re-oiled each day; and tanks 6, 7, 9, 10, and 12 were oiled on 4 May 1993 and allowed to weather.

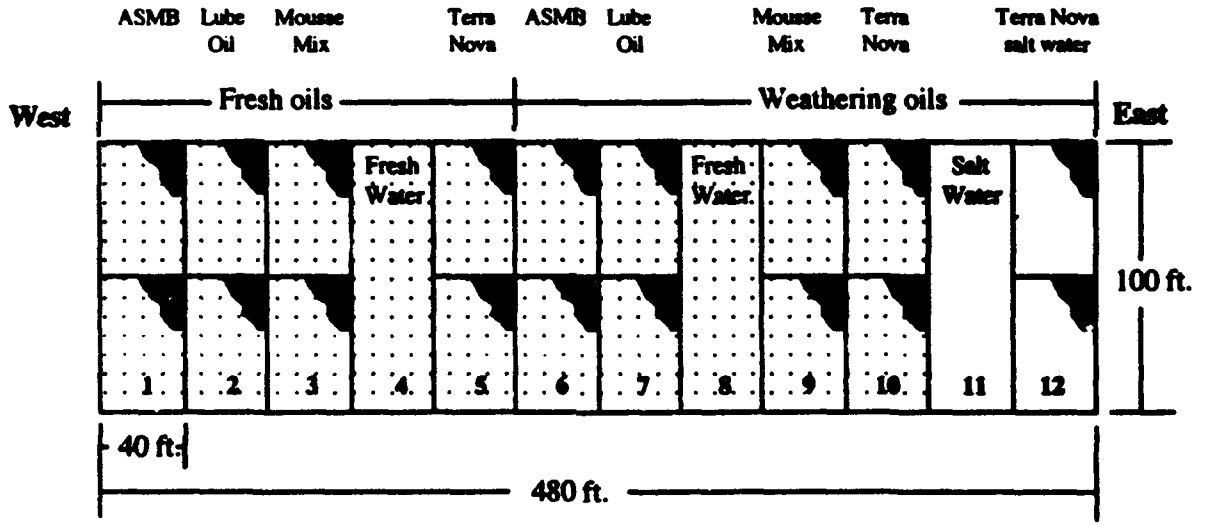

OIL TYPES

ASMB - Alberta Sweet Mixed Blend (a dark colored crude oil)
Lube Oil - Red hydraulic fluid (ESSI XD3-10)
Terra Nova - Dark colored crude oil
Mousse Mix - Dark colored mixture of ASMB and Bunker-C heavy fuel oil

Figure 1-1. Petawawa Test Facility

Table 1-2. Oil Time and Quantity Release Schedule

		ASMB	LUBE	MOUSSE MIX	WATER	TERRA NOVA	ASMB	LUBE	WATER	MOUSSE MIX	TERRA NOVA	SALT WATER	TERRA NOVA
	POOL #	1	2	3	4	5	6	7	8	9	10	11	12
Day 1	Morning	23	23	23	na	23	416	416	na	416	416	na	416
	Noon	68	68	68	na	68			na			na	
	Total	91	91	91		91	416	416	na	416	416	na	416
Day 2	Morning	91	91	91	na	91			na			na	
	Total	182	182	182		182	416	416	na	416	416	na	416
Day 3	Morning	416	416	416	na	416			na			na	
	Noon	416	832	416	na	624			na			na	
	Total	1014	1430	1014		1222	416	416	na	416	416	na	416

Notes:
1. Oil quantities are given in liters
2. Morning oil discharges were made at approximately 6:30 AM.
3. Noon oil discharges were made at approximately 11:30 PM.

1.4.2 Experiment Design and Conduct

Within the time slots allotted to the USCG, the R&D Center Test Director scheduled aircraft flight times and altitudes. R&D Center data collectors were onboard each of the participating aircraft to record data collection activities and to ensure that the desired image data sets were obtained. Table 1-3 provides a list of Coast Guard aircraft and the sensors they employed.

The HH-60J was assigned altitudes of 300, 500, and 1200 feet. The HH-60J was to orbit the test bed at each altitude to acquire imagery of the same scene from each onboard sensor. The HU-25B flew daytime passes over the test tank at altitudes of 500, 1000, and 1500 feet and nighttime passes at 1000 and 1500 feet. The HU-25B's nadir-looking line scanner imaged the tank only when directly overhead. The HU-25C flew daytime and nighttime passes at altitudes of 500, 1000, and 1500 feet. The HU-25C acquired FLIR and television (daytime only) sensor data on approach, while over the tanks, and as much as possible once past the tanks.

Table 1-3. Participating Coast Guard Units

UNITS	HOME BASE (Air Station)	SENSORS
HU-25B AIREYE	Cape Cod	RS-18C UV/IR line scanner
HU-25C	Miami	WF-360TL: FLIR & TV camera (day)
HH-60J	Traverse City	AGEMA 210 IRC-160ST FLIR 2000 FSI PRISM OWL (night) S-VHS (day)

1.5 RANGE OF ENVIRONMENTAL PARAMETERS ENCOUNTERED

Six potentially-significant atmospheric parameters were recorded by Environment Canada personnel during all sensor flights. The full list of these readings has been provided to the R&D Center for post experiment image analysis. The data were obtained at two identical stations, one at the east end and one at the west end of the test area. The range of atmospheric parameters encountered during the USCG time slots is provided in table 1-4. The atmospheric parameters and their units of measure were:

Temperature - Degrees Celsius (°C),
Relative humidity - Percent (%),
Wind speed - Kilometers per Hour (km/hr),
Wind direction - Degrees Magnetic (°M),
Barometric pressure - Kilopascal (kPa), and
Solar panel output - measured on a relative scale from 0 to 1400.

Those items designated as "Data Suspect", include east weather station air temperatures in excess of 80°C and negative values for relative humidity. The wind readings from the east and west stations were often significantly different. Wind readings taken from the west station were most likely affected by a small hill just west of the test site.

In addition to the atmospheric parameters listed in table 1-4, water temperature data were taken in each of the test tanks once during each sortie. The data were obtained from alternating north and south tanks by probes located at a water depth of approximately 1 cm. These data are provided in table 1-5. The times provided for each day are the approximate time that the temperatures were obtained. It should be noted that the temperature data were always obtained at the same location within a given tank, and this location varied from tank to tank. Depending upon the prevailing winds and oil quantity present during each round of temperature readings, some probes were beneath an oil layer while others were not.

Table 1-4. Range of Atmospheric Parameters Encountered

WEST STATION						
Time Slot	Air Temp(°C) Range (Average)	Rel. Hum.(%) Range (Average)	Wind Spd. (km/hr) Range (Average)	Wind Dir. (°M) Range (Average)	Barometer (kPa) Range (Average)	Solar Panel* Range (Average)
May 4 Day 1400-1700	17.8-18.1 (18.4)	59-63 (60)	0.3-7.3 (2.4)	145-235 (182)	102.1-102.4 (102.2)	1245-1250 (1246)
May 4 Night 2000-2300	15.9-17.8 (16.9)	64-74 (68)	0.2-3.5 (1.4)	135-195 (162)	102.3-102.7 (102.5)	2-962 (84)
May 5 Day 1400-1700	21.0-26.1 (24.0)	58-86 (74.7)	0.6-1.6 (1.0)	151-313 (226)	100.4-101.8 (101.1)	1239-1278 (1261)
May 5 Night 2000-2200	20.8-25.9 (22.4)	80-88 (83)	0.2-7.4 (2.1)	270-007 (329)	102.1-102.5 (102.3)	1-955 (186)
May 6 Day 1400-1700	18.3-22.2 (20.6)	31-49 (37.3)	5.6-14.2 (10.1)	262-036 (358)	101.3-102.1 (101.7)	1294-1321 (1310)
EAST STATION						
Time Slot	Air Temp(°C) Range (Average)	Rel. Hum.(%) Range (Average)	Wind Spd. (km/hr) Range (Average)	Wind Dir. (°M) Range (Average)	Barometer (kPa) Range (Average)	Solar Panel* Range (Average)
May 4 Day 1400-1700	15.9-16.3 (16.1)	59-60 (59)	7.3-22.2 (13.1)	141-217 (179)	102.5-102.7 (102.6)	1219-1225 (1222)
May 4 Night 2000-2300	15.9-18.9 (17.4)	60-67 (63)	1.6-15.2 (6.4)	108-202 (148)	102.5-102.8 (102.6)	2-1066 (93)
May 5 Day 1400-1700	Data Suspect	58-78 (69)	0.6-17.5 (6.0)	179-316 (243)	101.1-102.0 (101.6)	1214-1246 (1232)
May 5 Night 2000-2200	Data Suspect	74-80 (76)	5.0-14.9 (7.9)	306-000 (334)	102.3-102.5 (102.4)	2-1036 (200)
May 6 Day 1400-1700	Data Suspect	Data Suspect	8.6-33.0 (19.0)	307-012 (342)	102.3-102.1 (102.0)	1271-1296 (1286)

* Solar panel output was measured on a relative scale from 0 to 1400.

Table 1-5. Test Tank Water Temperatures

	TANK NUMBER											
	1	2	3	4*	5	6	7	8*	9	10	11*†	12†
	Fresh Oil (deg. C)					Weathered Oil (deg. C)						
May 4 Day 14:50	16.7	16.5	16.8	16.9	17.7	16.9	19.6	16.7	16.6	17.1	16.4	17.6
May 4 Night 20:40	16.7	16.5	16.4	16.2	16.7	16.6	16.9	16.3	16.5	16.4	16.1	16.4
May 5 Day 14:30	16.9	17.3	16.7	16.9	18.6	16.9	20.3	17.2	16.9	16.9	17.0	21.6
May 5 Night 21:05	18.8	18.2	18.5	18.0	18.2	18.7	18.2	18.2	18.7	17.9	18.1	18.6
May 6 Day 14:20	22.0	22.7	21.3	21.9	21.3	24.9	21.2	21.1	21.5	20.5	21.0	23.8

* indicates water only tanks
† salt water base (all other tanks are fresh water based)

1.6 IMAGE DATA PREPARATION

1.6.1 Creation of Infrared Video Imagery

Video tapes of the IR sensor imagery were reviewed to identify which segments provided the most representative demonstration of operational sensor performance. In selecting representative frames from the helicopter imagery, an effort was made to obtain images from the same altitude and look angle for comparative evaluation across sensors. The selected video frames were extracted from the original S-VHS video tapes, using an S-VHS video cassette player/recorder and digitized using a video capture board providing input to an IBM PC-compatible 486/DX desktop computer. These images were saved initially in 24-bit color bit-mapped (BMP) format, imported directly to ALDUS PhotoStyler software for conversion to 8-bit gray-scale TIFF files, and processed as described below. The PhotoStyler software was used to adjust the image brightness and contrast to best display image features, then to print the image to a Kodak XLT-7720 digital continuous tone printer. The result was a high-quality print of each selected image. The IRC-160ST display is 10-bit, and conversion to 8-bit for computer manipulation loses some of the dynamic range or sensitivity available with the sensor; however, image quality remains reasonable close to that available directly with the sensor.

When a video tape is playing, the scene is continuous and the observer must integrate a series of individual image frames into an understandable moving picture. During normal playback, video noise on a television monitor is integrated over successive frames at a rate such that the human viewer perceives a clearer, more detailed image than is available in a single video frame. When the video tape is stopped or slowed to the point where individual frames can be viewed, the image quality is often significantly worse than the perceived quality in the moving video. Since only single video frames could be captured and digitized for analysis, a method for simulating the real-time sensor image quality was employed when individual frames were judged to be of low fidelity. This method required that two video frames be captured and summed. Typically these were successive frames; however, if successive frames could not provide satisfactory single-frame image quality, video frames in close time proximity were captured.

To construct the simulated real-time images, each pair of captured video frames was opened in Atlantis Scientific Systems' EarthView software. This software was used to coregister important scene features (such as the test tank) in the image pairs so that they overlapped exactly. The pixel gray scale values in each frame were then divided by two and the images were summed. This frame manipulation had the net effect of strengthening actual image features and reducing some of the noise, thereby resulting in a "best approximation" to the image perceived in the moving video. Where sensor information (cross hairs, tuning status bar, etc.) was superimposed on some of the infrared images, the coregistration of scene features and subsequent frame summation sometimes blurred or created a double of the superimposed information. This effect, while annoying to look, at did not adversely affect the quality of the infrared images. The summed images were saved to 8-bit TIFF files and opened in PhotoStyler for final processing and printing.

1.6.2 Visible Spectrum Reference Images

Figure 1-2 provides sample images of video camera output from the S-VHS camera (top) and WF-360TL TV camera (bottom). Both images show the test bed and sand berms separating the tanks. Both images also show some of the differences in the oil types. The lube oil, for example, is a lighter color than each of the other oils. In all cases, the video images compared favorably with higher resolution still photographs taken during the experiment. Unlike the infrared systems, these cameras record reflected energy in the visible spectrum only, requiring an illumination source such as the sun. They are prone to degradation by low levels of ambient lighting, poor visibility, or when strong specular reflections, such as sun glitter, are in the line of view. Since the infrared sensors detect blackbody radiation emitted by the objects in the scene as well as available reflected energy (present primarily in the MWIR band), they will not always show the same oil-water boundaries as the visible spectrum reference data.

A. S-VHS Camera, 5 May 1993, 300 ft

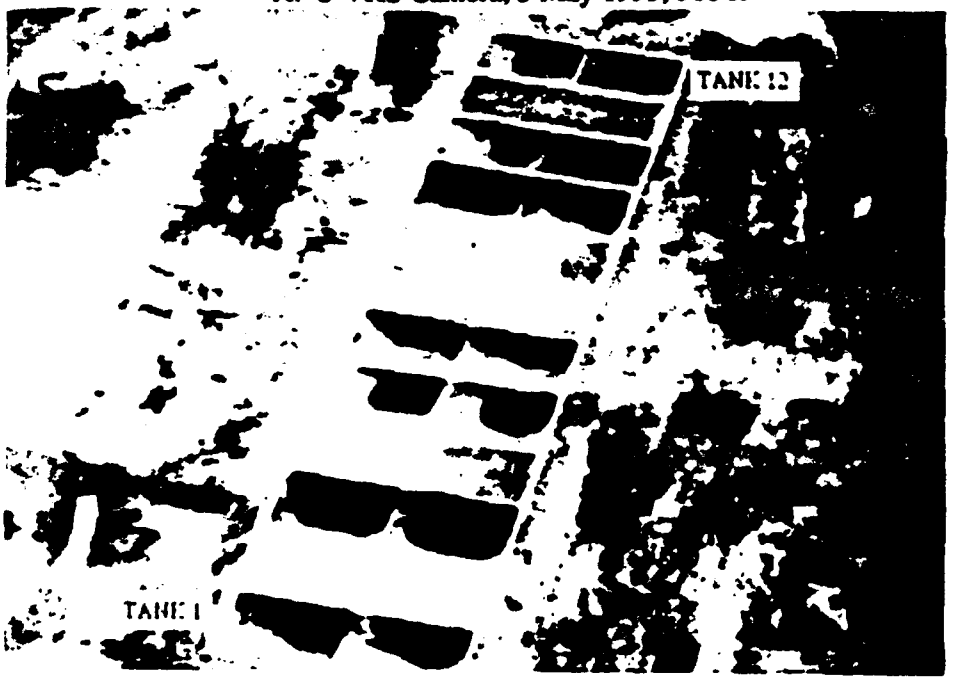

B. WF-360 TV Camera, 5 May 1993, 1000 ft.

Figure 1-2. Sample Daytime Visible Spectrum Imagery

Figure 1-3 provides a sample image from the Dark Invader Owl NVG camera under overcast, moonlit conditions. As with the daytime video imagery, the Dark Invader Owl camera image depicts the test tank, test tank outlines, and differences in brightness among the oils. However, high or low ambient lighting, bright light point sources, or low battery power to the light amplification tube can adversely affect image quality. Since this sensor operates in the visible and slightly into the near IR spectrum, it is subject to environmental constraints similar to those cited above for the daylight video cameras.

When viewing this visible spectrum reference imagery, caution must be observed. The water in the test tanks was only 6 inches deep, and while the MWIR and LWIR wavelengths penetrate only centimeters, the wavelengths associated with visible light can easily penetrate water of this depth. Thus, the non-oiled sections of the tank are reflecting visible energy off the bottom which does not contrast with the oil in the same way that a deeper ocean background would. Since the test tank water was optically deep to the IR imagers, bottom reflections did not influence their imaging performance in this way.

This artifact of the test environment resulted in visible-spectrum images that provided excellent, but misleading, contrast between oiled and clean portions of the test tank. The reader is cautioned that the surface truth images presented in this report, while providing useful comparisons to the IR data, are not necessarily representative of the oil/water contrast expected in the operational environment. This is expected to be especially true for the night imagery, as is illustrated below.

Figure 1-3. Sample Dark Invader Owl Imagery, Night, 5 May 1993, 300 ft.

Figure 1-4, which depicts an image from the Dark Invader Owl on the night of 5 May 1993, illustrates the shallow water's effect on oil/water contrast. This image includes a portion of the lake that is located just south of the test site. In figure 1-4, a line has been superimposed through the north and south sections of tank 9, over the ground, and into the lake, ending approximately 40 feet from shore. This line is labeled "lake line". The bottom half of figure 1-4 provides a line plot of pixel intensity (y-axis) versus pixel number (x-axis) for the image along this line. It is clear from this plot that the lake water is significantly darker than the water in the test tank, and even the dark oils appear somewhat lighter than the lake water. Had the oil been discharged on the lake, it is not clear that sufficient contrast would have existed at night to differentiate between oil and the deeper water using the NVG camera.

1.7 IMAGE ANALYSIS OVERVIEW

Chapters 2 and 3 present the results of analyses conducted on the captured IR imagery. Chapter 2 presents imagery from each of the sensors, and provides a qualitative review, while chapter 3 presents a more quantified analysis of specific images. Where available, captured visible spectrum video imagery is used to provide surface truth comparisons.

For the more qualitative analysis of chapter 2, imagery for both video polarities (black = hot and white = hot) will be presented for each IR imager. Both night and day images will be presented. Samples of the best imagery from each sensor will be presented in a manner that will enable the reader to evaluate different imagers under comparable date, time of day, altitude, and look direction conditions. Sensor ergonomics are discussed based on operator comments and representative imagery.

In chapter 3, where selected image sets are evaluated side-by-side, a summary of atmospheric conditions and sensor parameters is provided for each image set. Where available, test tank water temperatures are also included. Comparisons are made among the MWIR hand-held systems, among LWIR installed sensors, and between the MWIR and LWIR sensors. In selected images, oil slick surface areas were measured to develop oil thickness estimates. Concurrent IR and visible spectrum images were obtained, where available, for these analyses.

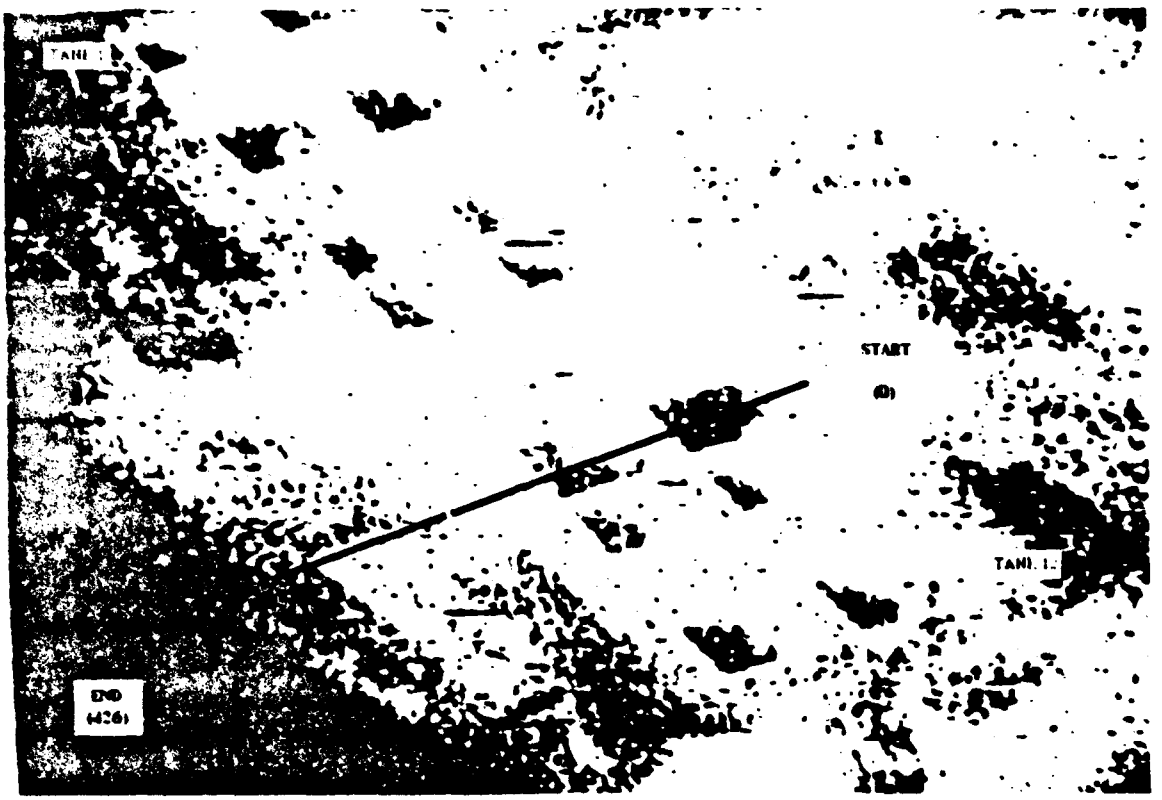

A. Dark Invader Owl Image, 5 May, 1993

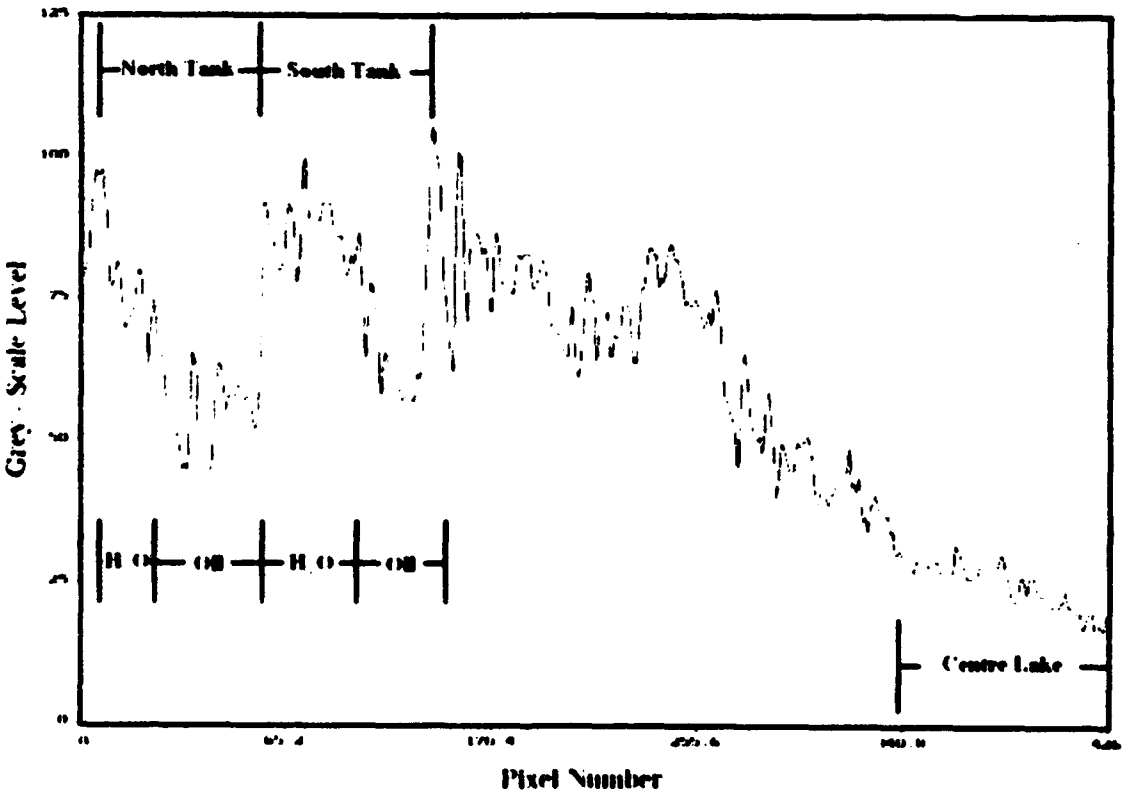

B. Intensity Plot of Lake Line in Dark Invader Owl Image

Figure 1-4. Investigation of NVG Pixel Intensity

CHAPTER 2
IMAGERY OVERVIEW

This chapter introduces imagery from each sensor evaluated during the Petawawa field test. Table 2-1 summarizes the image data obtained from each of the sensors. Section 2-1 presents representative, visible-spectrum surface truth imagery and describes the environmental factors that existed during each sortie. Section 2.2 presents MWIR imagery and section 2.3 presents LWIR imagery from selected sorties. Where possible, images from the same date, time of day, altitude, and look direction are presented for each imager; however, an example of the best imagery obtained from each imager has been chosen to provide a perspective of the optimum sensor performance. Section 2.4 discusses man-machine interface (MMI) considerations for each of the hand-held sensors used. These are based on operator comments during testing and imagery that illustrates specific operability issues.

2.1 SURFACE TRUTH DATA

As discussed in Chapter 1, daytime video and nighttime NVG camera imagery were captured to provide surface truth data. Due primarily to changing wind direction and the inability to obtain continuous surface truthing, image-for-image comparison of visible and IR imagery is not possible except for the daytime WF-360TL data. Visible spectrum imagery is presented below to provide representative views of the size, shape, and position of each oil slick within the test tank during the IR imaging activities. With each visible spectrum image, a brief description of the environmental factors which affected IR imaging during the sortie is presented. These descriptions are based on the same data that table 1-4 was derived from.

Figure 2-1 provides daytime imagery from 4 May 1993. Frame "a" is from the S-VHS camera on board the HH-60J and frame "b" is from the WF-360TL TV camera.

The daytime sortie on 4 May 1993 had clear skies with a relative humidity around 60 percent and winds predominantly out of the south. Recorded air temperatures were roughly 16°C at the east weather station and about 18°C at the west station.

Figure 2-2 provides daytime imagery from 5 May 1993. Frame "a" is from the S-VHS camera on board the HH-60J and frame "b" is from the WF-360TL TV camera.

The daytime sortie for 5 May 1993 had overcast conditions with scattered rain showers. Wind speeds were generally low (0.6-1.6 km/h) and at the west station varied between southerly and westerly directions while at the east station more of an actual wind shift from southerly to westerly was recorded. During this sortie, the roughly 80 percent relative humidity at the start of the sortie dropped to about 60 percent by the end of the sortie and the barometric pressure continued its day-long drop. Air temperatures rose from a low of 21.0°C to a high of 26.1°C during the USCG sorties.

Figure 2-3 provides daytime imagery from 6 May 1993. Frame "a" is from the S-VHS camera on board the HH-60J and frame "b" is from the WF-360TL TV camera.

The 6 May 1993 sortie was very bright and sunny. This was the clearest day of the field test and air temperatures ranged between 18.3°C and 22.2°C during the USCG sorties. Storms from the previous day were gone and the air coming out of the northwest was dry. Relative humidity dropped from 50 percent to a low near 30 percent towards the end of the sortie. Winds varied between the northeast and northwest at moderate (5.6-14.2 km/h) speeds.

Oil was added to tanks 1, 2, 3, and 5 each day of the test; therefore, on the day of the 6th, these tanks contained the most oil and provided the best images of the oil.

Figure 2-4 provides nighttime imagery from the Dark Invader Owl on 4 May 1993.

The nighttime sortie for 4 May 1993 was characterized by a clear sky and a near full moon. Wind speeds were somewhat variable, but tended to be out of the southeast. Air temperatures dropped from roughly 18°C to around 16°C over the course of this sortie, and the relative humidity rose from 60 to 70 percent.

Figure 2-5 provides nighttime imagery from the Dark Invader Owl on 5 May 1993.

By nightfall on 5 May 1993, the showers had stopped; however, it was still overcast and the humidity had gone back up to 80 to 90 percent by the end of the sortie. The winds were generally light (0.2-7.4 km/h) and variable out of the northwest. The air temperature this night ranged from 20.8°C to 25.9°C (approximately 6 degrees warmer than the night of the 4th).

Table 2-1. Summary of Altitudes* At Which Sensor Imagery Were Obtained

TIME FRAME	SENSOR														
	AGEMA 210		IRC-160ST		FSI PRISM		FLIR 2000		WF-360TL IR & TV		RS-18C			VIDEO	OWL NVG CAMERA
	WH†	BH††	WH†	BH††	WH†	BH††	WH†	BH††	BH††	WH†	IRLO	IRHI	UV		
MAY 4 DAY	300 500 1200	300 500 1200	300 500 1200	300 500 1200	300 500 1200	300 500 1200	300 500 1200	300 500 1200	500 1000 1500	500 1000 1500				300 500 1200	
MAY 5 DAY	300 1200	300 500 1200	300 500 1200	300 500 1200			300 500 1200	300 500 1200	500 1000 1500	500 1000 1500	500 1000 1500	500 1000 1500	500 1000 1500	300 500	
MAY 6 DAY	300 500 1200	300 500 1200	300 500 1200	 500 1200			300 500 1200	300 500 1200	500 1000 1500	500 1000 1500	500 1000 1500	500 1000 1500	500 1000 1500	300 500 1200	
MAY 4 NIGHT	 500 1200	 500 1200	 1200	 1200	 500 1200	 500 1200	300 500 1200	 500 1200	500 1000 1500	500 1000 1500					Various
MAY 5 NIGHT			300 500 1200	300 500 1200			300 500 1200	300	500 1000 1500	500 1000 1500	1000 1500	1000 1500	1000 1500		Various

* Altitude provided in feet

† White = Hot video polarity

†† Black = Hot video polarity

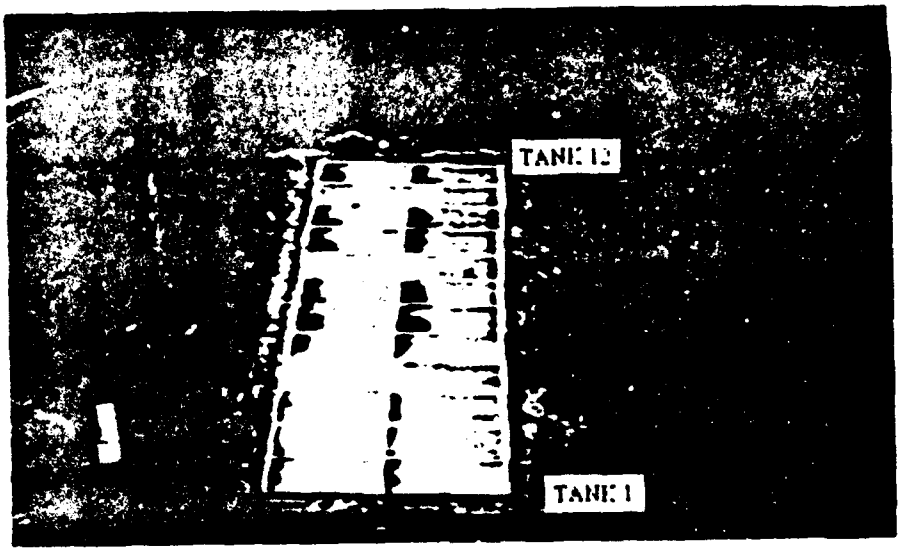

A. S-VHS Camera

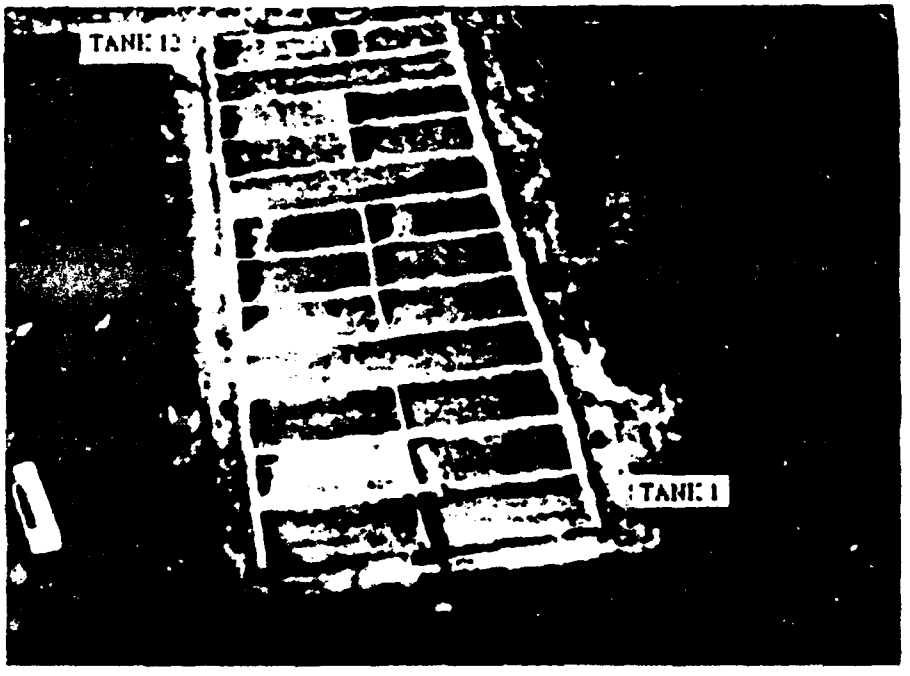

B. WF-360TL TV Camera

Figure 2-1. Daytime Visible Spectrum Imagery, 4 May 1993

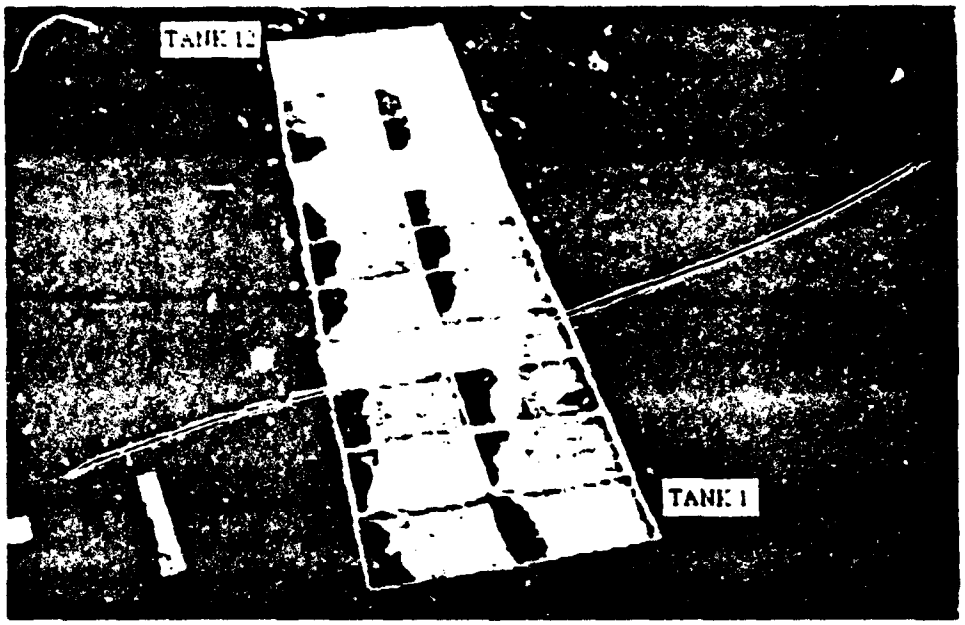

A. S-VHS Camera

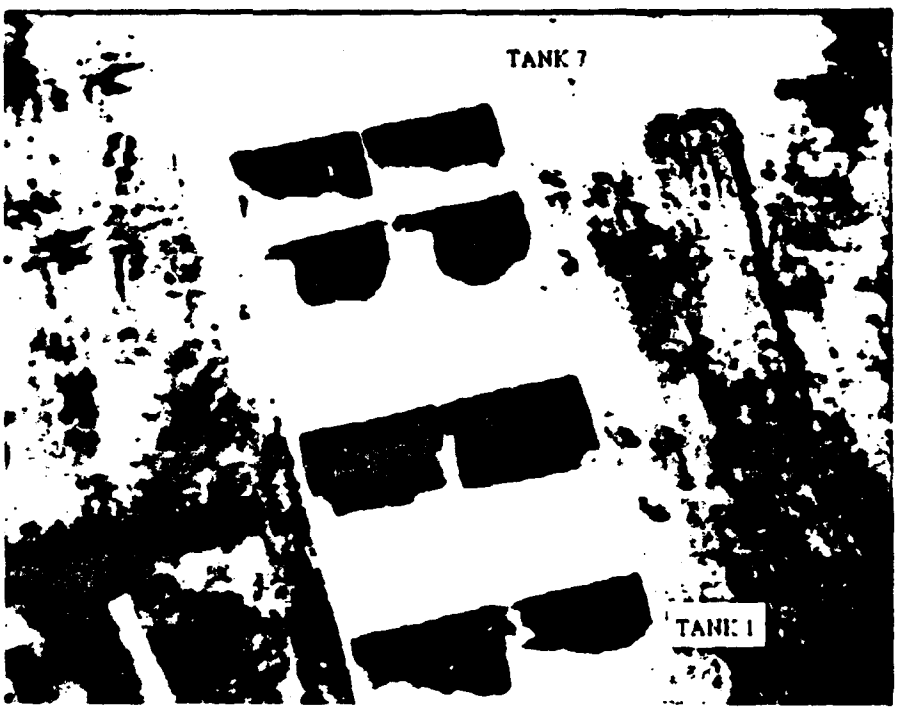

B. WF-360TL TV Camera

Figure 2-2. Daytime Visible Spectrum Imagery, 5 May 1993

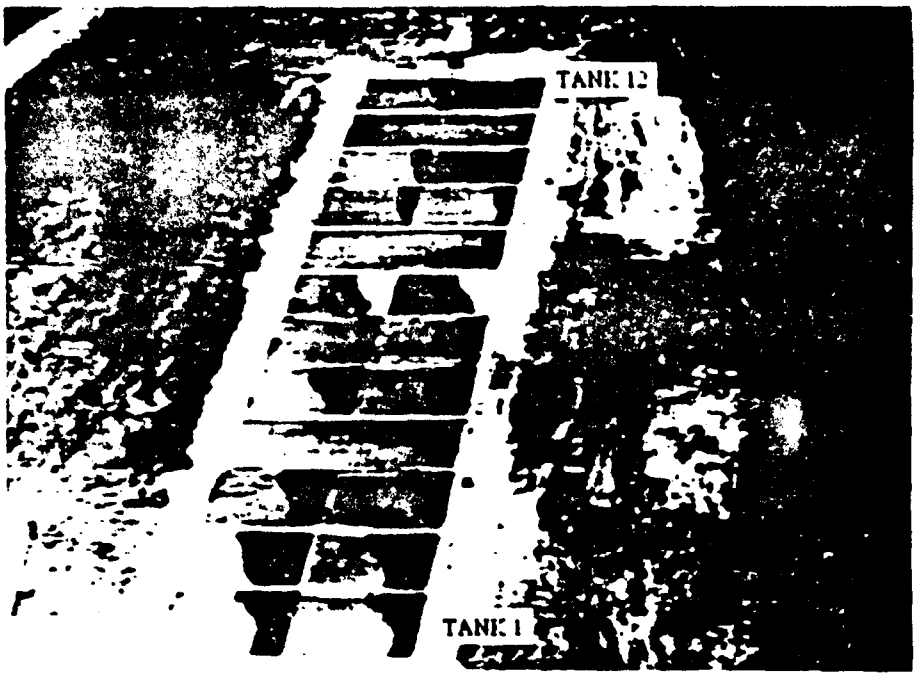

A. S-VHS Camera

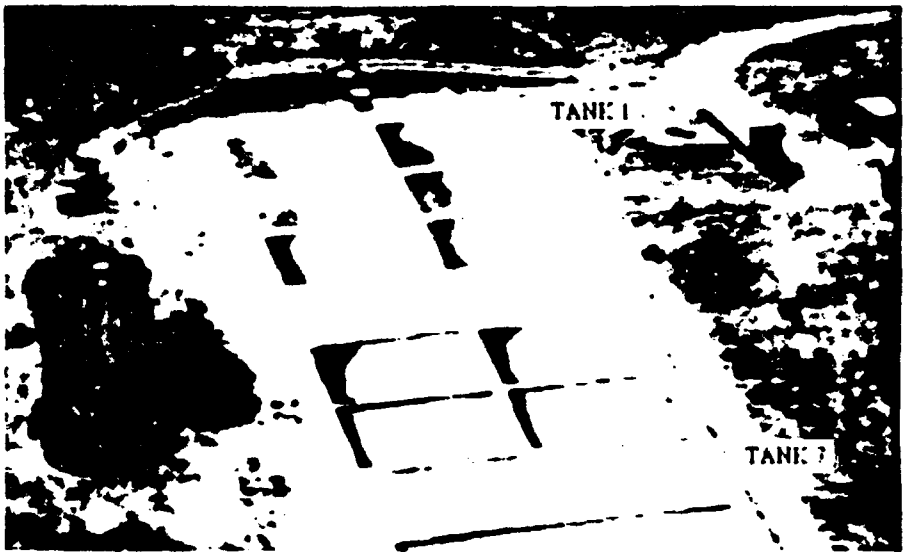

B. WF-360TL TV Camera

Figure 2-3. Daytime Visible Spectrum Imagery, 6 May 1993

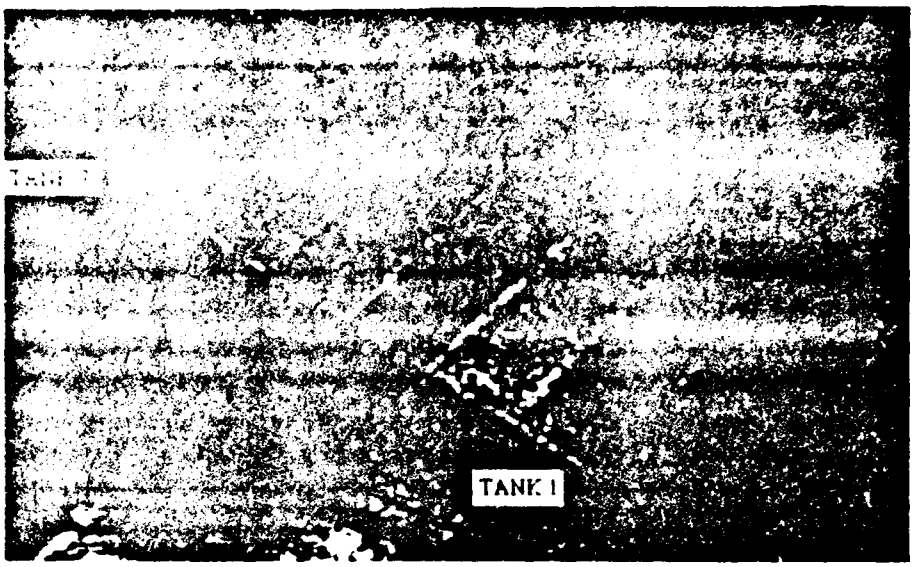

Figure 2-4. Dark Invader Owl Imagery, 4 May 1993

Figure 2-5. Dark Invader Owl Imagery, 5 May 1993

2.2 REPRESENTATIVE IMAGERY FROM HAND-HELD MWIR SENSORS

The MWIR sensors tested are hand-held sensors with fixed lens capabilities. Although the IRC-160ST and FSI Prism provide the ability to change lenses (50-and 25-mm lenses were available during the test), the 25mm lens imagery was limited, and only 50mm imagery will be presented here. All three imagers permit the operator to switch video polarity at will between black = hot and white = hot.

Each MWIR sensor demonstrated the ability to detect oil on water in a daytime environment. The ability of MWIR sensors to detect an oil/water contrast during the night sorties was marginal and apparently sensitive to environmental factors, particularly the ambient temperature.

In the daytime images the lube oil appears cooler than the other oils, probably due to its red color which is less efficient than the black crudes and bunker oil at absorbing solar energy. At night, when differential heating was not present, thermal contrast between the each of the oils and the water was more uniform.

2.2.1 Daytime MWIR Images

Figures 2-6 through 2-8 are MWIR images taken at 300-foot altitude during the 4 May daytime sortie. All three hand-held MWIR sensors are represented in this image set, with frame "a" in each figure depicting white = hot video polarity and frame "b" depicting black = hot polarity. Figure 2-6 through 2-8 depict good oil/water contrast in spite of overcast conditions, with the oil pushed by a southerly wind up against the northern boundary of each test tank cell.

The 4 May images provide for direct comparison of all three MWIR sensors, but they are not the highest quality MWIR images obtained. Imagery from 6 May demonstrates the ability of these sensors to depict oil slicks when oil/water thermal contrast is very high due to strong differential solar heating. Unfortunately, the FSI Prism was not available on the 6 May sortie due to a broken power supply connection.

Figures 2-9 and 2-10 present daytime imagery from the Agema 210 and the IRC-160ST, respectively. These images were taken on 6 May 1993 from an altitude of 500 feet. Again, both white = hot and black = hot video polarities are depicted for each sensor.

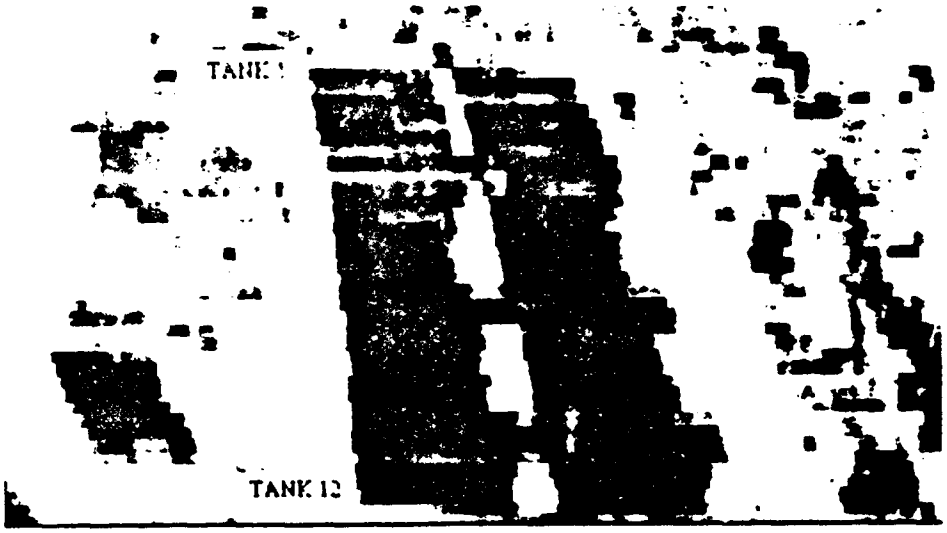

A. White Hot

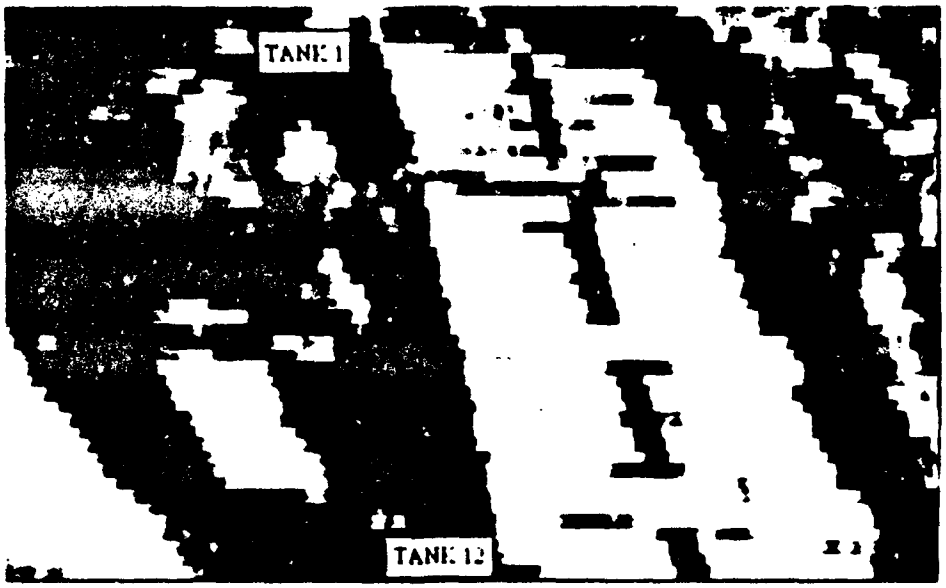

B. Black Hot

Figure 2-6. Agema 210, Daytime, 4 May 1993, 300 ft.
(best available images: over-contrasted by an inexperienced operator)

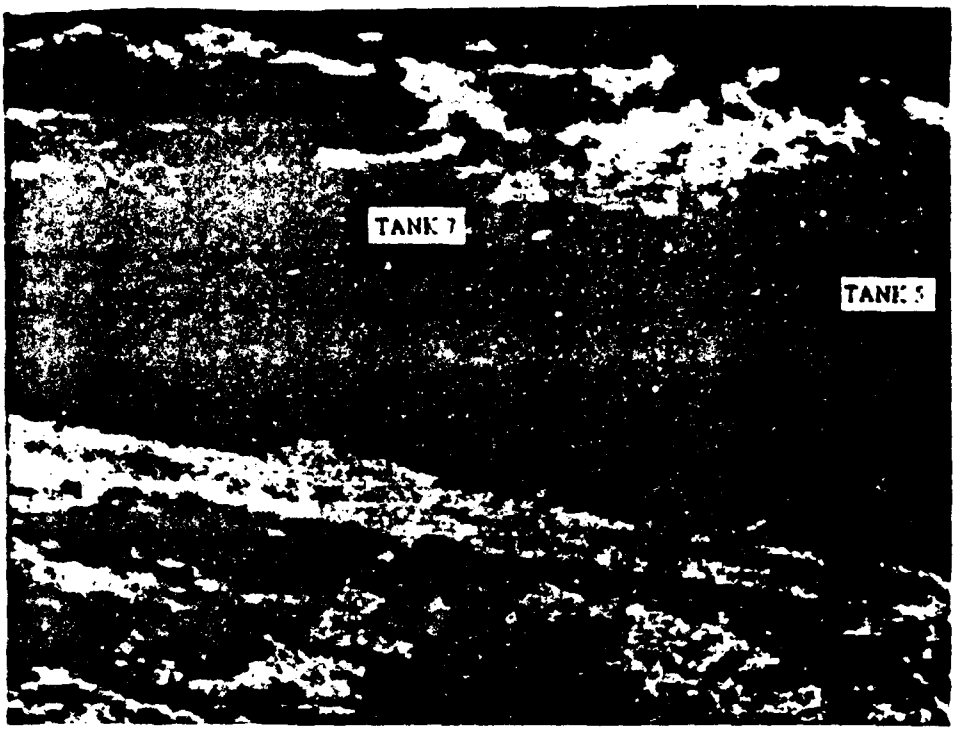

A. White Hot

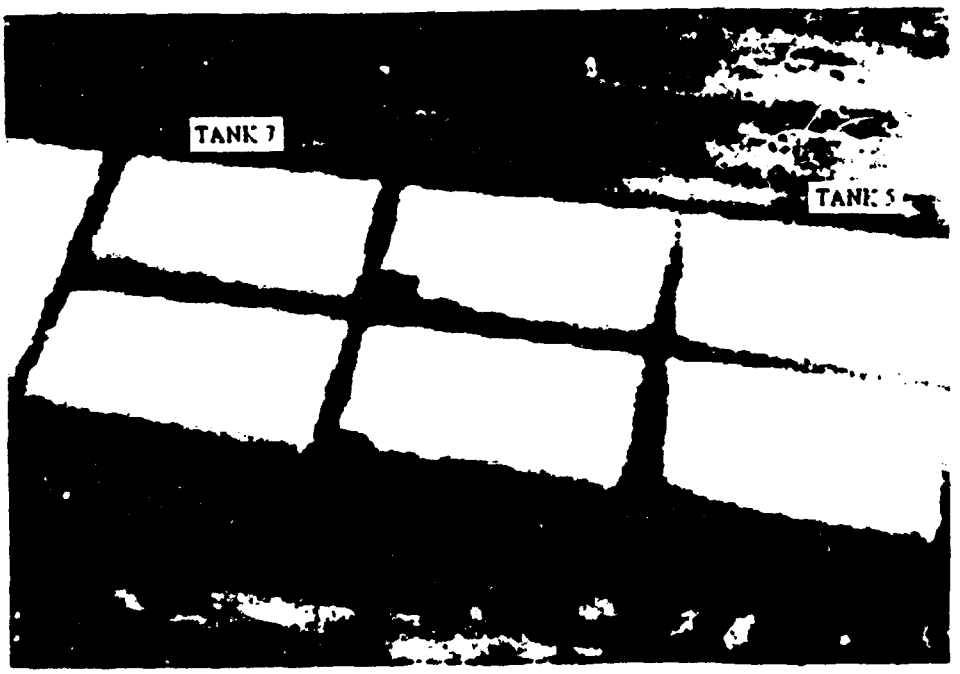

B. Black Hot

Figure 2-7. IRC 160ST, Daytime, 4 May 1993, 300 ft.

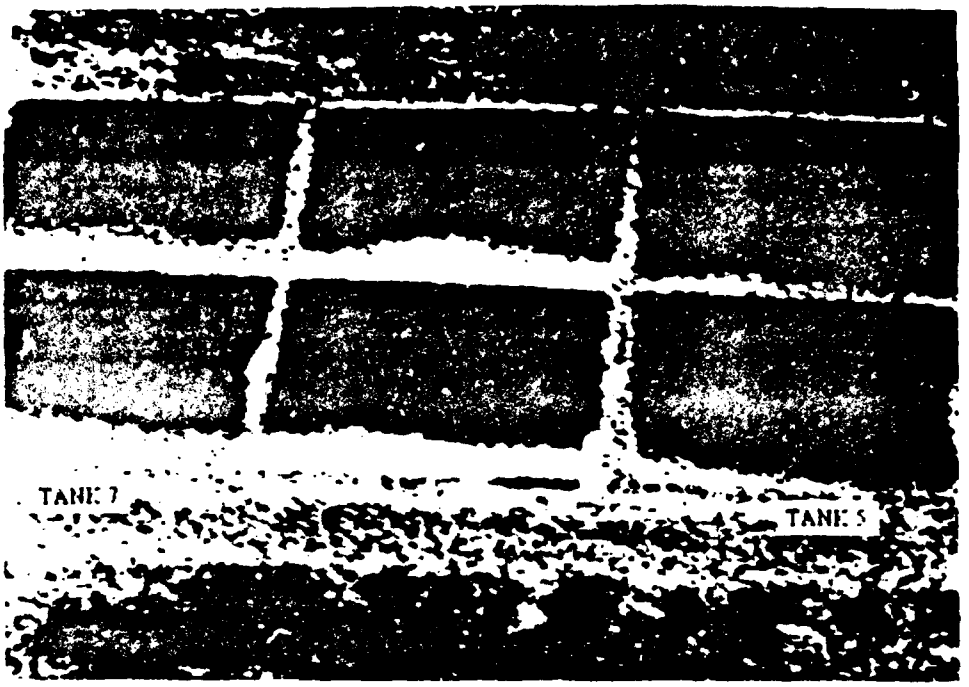

A. White Hot

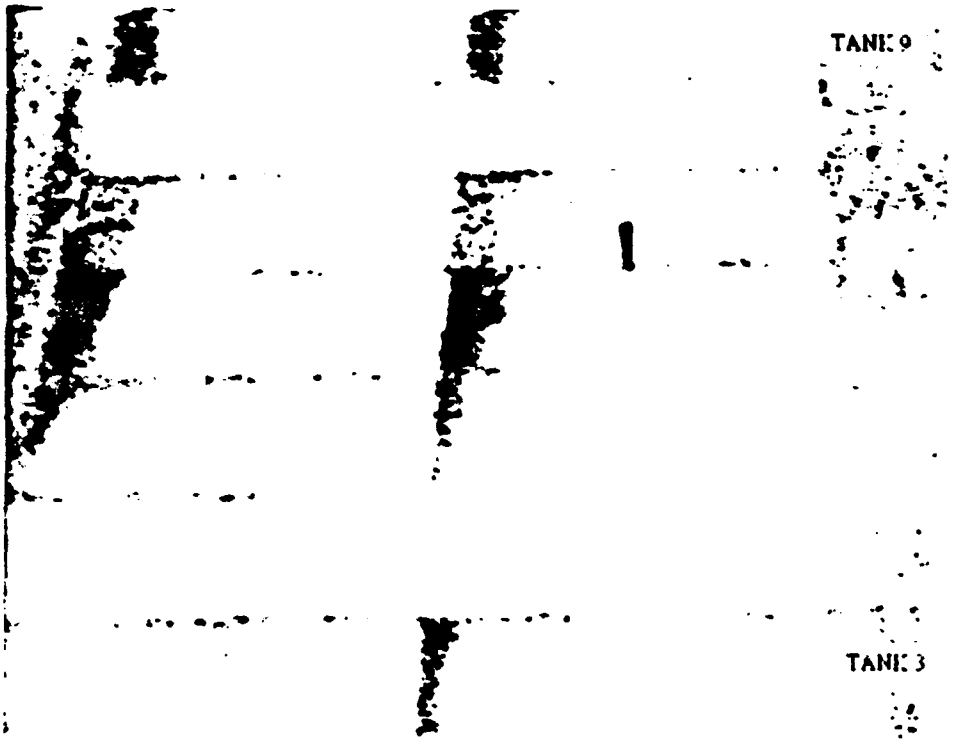

B. Black Hot

Figure 2-8. FSI Prism, Daytime, 4 May 1993, 300 ft.

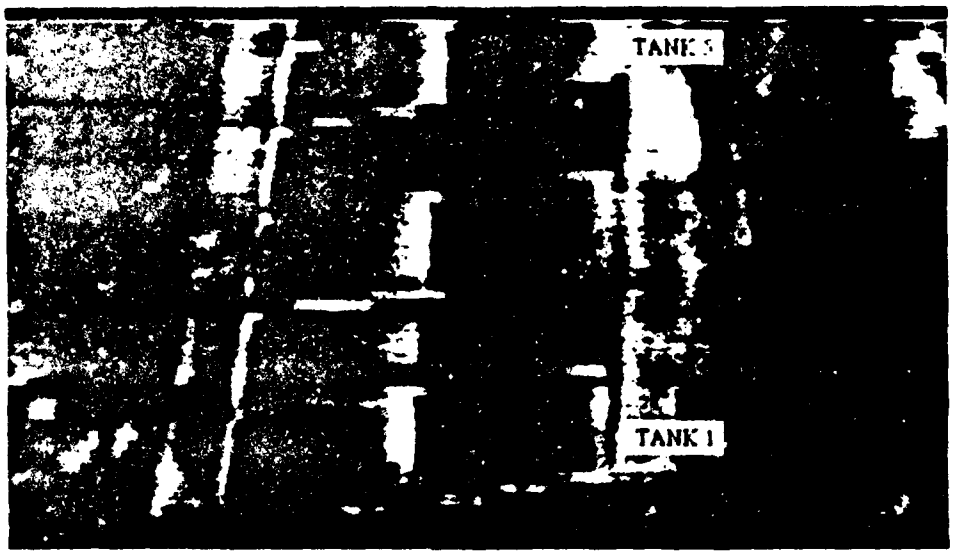

A. White Hot

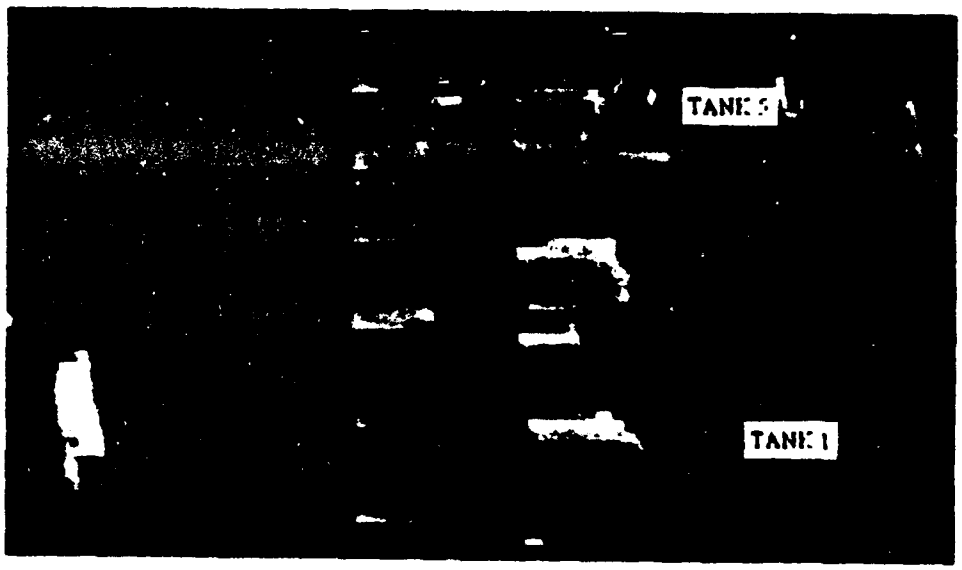

B. Black Hot

Figure 2-9. Agema 210, Daytime, 6 May 1993, 500 ft.

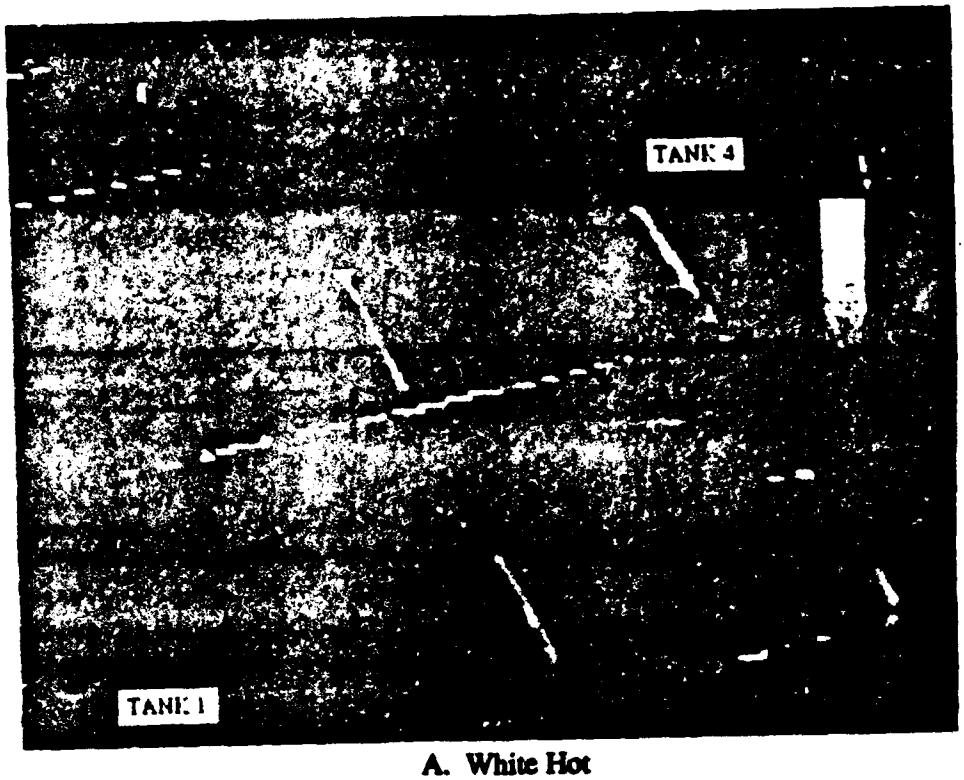

A. White Hot

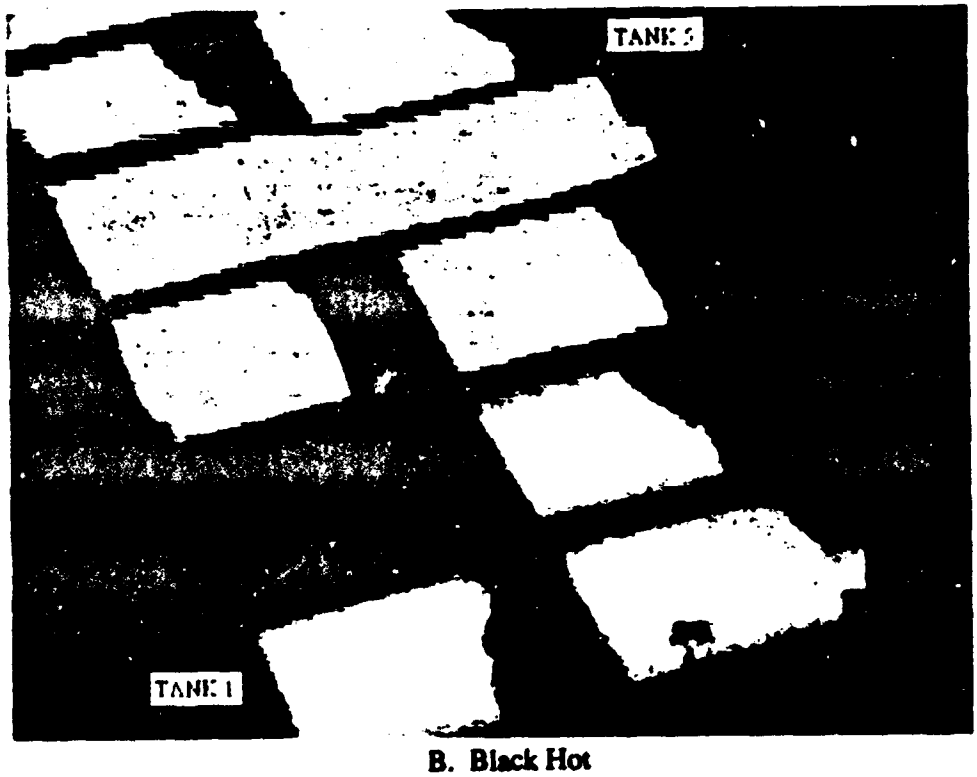

B. Black Hot

Figure 2-10. IRC 160ST, Daytime, 6 May 1993, 500 ft.

Discussion of Daytime MWIR Imagery

The lower pixel resolution of the Agema 210 (which is significantly cheaper and smaller than the other two hand-held sensors) resulted in blocky images which lacked fine spatial detail. The FSI Prism with its 256- by 256 element focal plane array, provided high spatial resolution in the images; however, system noise caused the images have the appearance of being taken through frosted glass. The IRC-160ST images, when properly tuned, were very clear. With an intermediate-resolution focal plane array of 160- by 120 elements, the IRC-160ST displayed a tendency to create a stepped look to linear features when the imager was tilted diagonally with respect to those features. The magnitude of this distortion was minor and did not detract significantly from image interpretability.

In a comparison of daytime MWIR and visible spectrum images, all imagers (visible and IR) depict the oil pushed against the north berm of the test tanks in the 4 May images and in the southern portion of the test tank in the 6 May images. The IRC-160ST and FSI Prism provided the ability to observe fine slick edge detail and depicted a distinct oil/water boundary. The images showing the most detail within the oil slicks are those in figure 2-10 from the IRC-160ST. Both images in figure 2-10 provide very good information about the thermal differences within the oil slicks. Slick edge shape and detail match well with the visible spectrum data shown in figure 2-3. With the Agema 210, the pixel resolution was too coarse to accurately depict slick edge details. Slick edge details provide important cues to the sensor operator when attempting to distinguish oil slicks from other phenomena (e.g. warm water outflows or upwellings) in an operational mission scenario.

Video polarity does not appear to affect the spatial resolution or clarity of the IR images. Although both black = hot and white = hot polarities are able to present the same quality image, some operators will find it easier to consistently distinguish oil/water contrast and slick edge details in one polarity simply because of their individual interpretations of visual cues. Switching from one polarity to the other did not appear to provide any advantage when the sensor operators attempted to obtain a clearer image.

2.1.2 Nighttime MWIR Images

Figures 2-11 through 2-13 are MWIR images taken at 1200-foot altitude during the 4 May nighttime sortie. All three hand-held MWIR sensors are represented in this image set, with frame "a" in each figure depicting white = hot video polarity and frame "b" depicting black = hot polarity.

None of the MWIR sensors were able to detect significant contrast between the oil and water on the night of 4 May. Although lower altitude data are sparse, those available do not indicate a significant improvement in contrast over the images shown here. On the warmer and more humid night of 5 May, the IRC-160ST was able to display fair oil/water contrast. This is demonstrated in figure 2-14, which presents IRC-160ST imagery taken from 1200 feet on the night of 5 May. Unfortunately, the Agema 210 and Prism sensors were not available for comparison on the 5 May nighttime sortie.

Discussion of Nighttime MWIR Imagery

The nighttime MWIR images obtained on 4 May (figures 2-11 through 2-13) appear to be properly tuned, but almost no oil/water contrast is visible. These images depict the sand berms, oil drums along test tank cells 1,2,3, and 5 (still warm from daytime heating) and the trailer site, but not the oil slicks in the test tanks. The images in figures 2-11 through 2-13 were all taken from a 1200-foot altitude and may not represent an ideal case; however, the low altitude MWIR imagery on the night of 4 May is very limited and does not indicate a significant improvement in the MWIR visibility of the oil slicks.

Figures 2-5 (NVG) and 2-14 (IR) are from the night of 5 May and both depict slicks concentrated in the southeast corner of the oiled cells. The oil/water contrast is stronger at lower altitude in the IRC-160ST imagery; however, it can still be seen from 1200 ft as shown in figure 2-14. Chapter 3, section 3.4 presents a discussion of the effects of altitude on image quality and FOV. Examples of nighttime images are included there. In figure 2-14, cells 6 and 7 (weathered oil) show a larger slick area than cells 1,2,3, and 5 (re-oiled daily). This generally agrees with the surface truth image features in figure 2-5.

As discussed in section 1.2, there is a minimal contrast threshold available in the MWIR spectral band. This minimal contrast means that relatively minor changes in path length, sensor settings, or environmental conditions can change whether the oil/water is detected. This is demonstrated in the images from nights of 4 May and 5 May.

False slicks were easily created in the night imagery from all three imagers while tuning for brightness and contrast during post experiment image analysis. Sensor operators must be familiar with tuning adjustments to prevent similar results in the field. Because of the nature of this experiment and the availability of readily-identifiable ground features to assist image tuning in this experiment, false positives where not a problem during field test use.

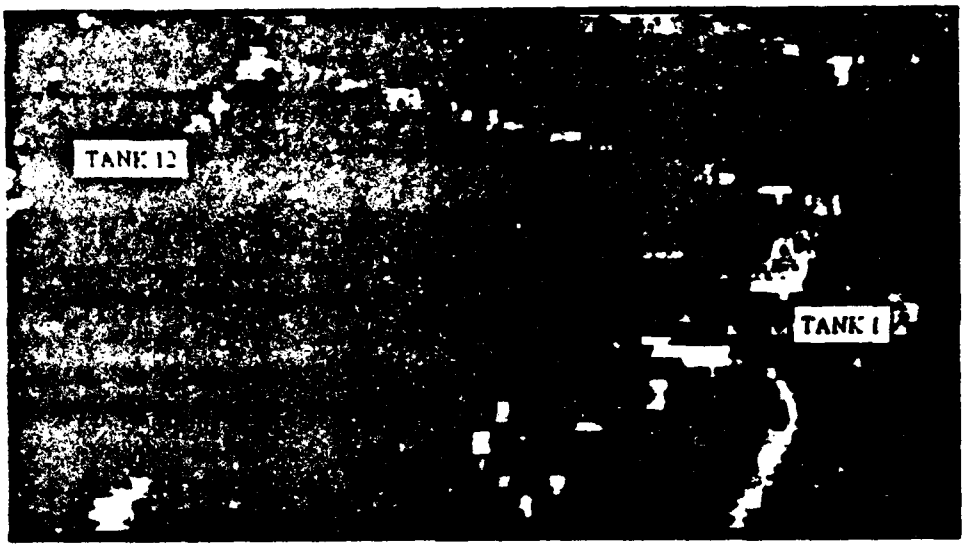

A. White Hot

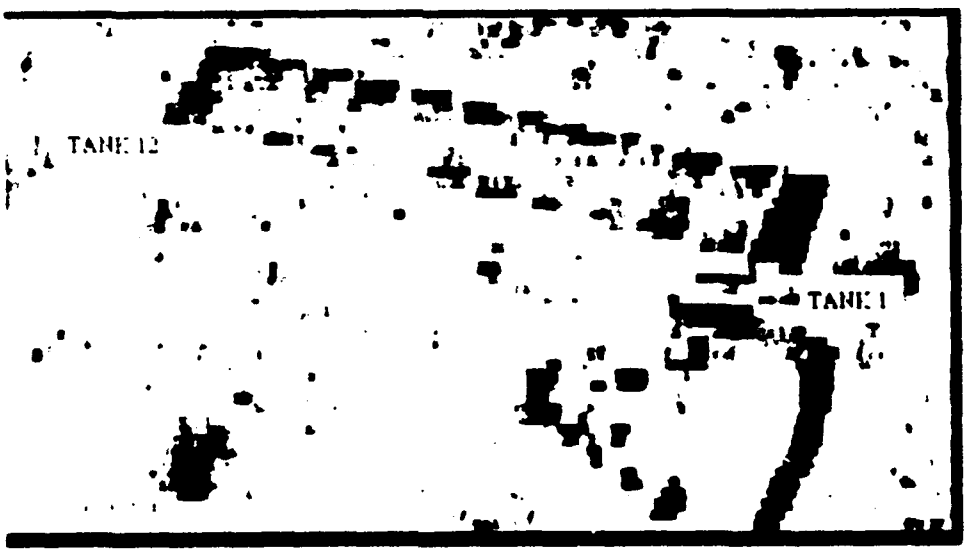

B. Black Hot

Figure 2-11. Agema 210, Nighttime, 4 May 1993, 1200 ft.

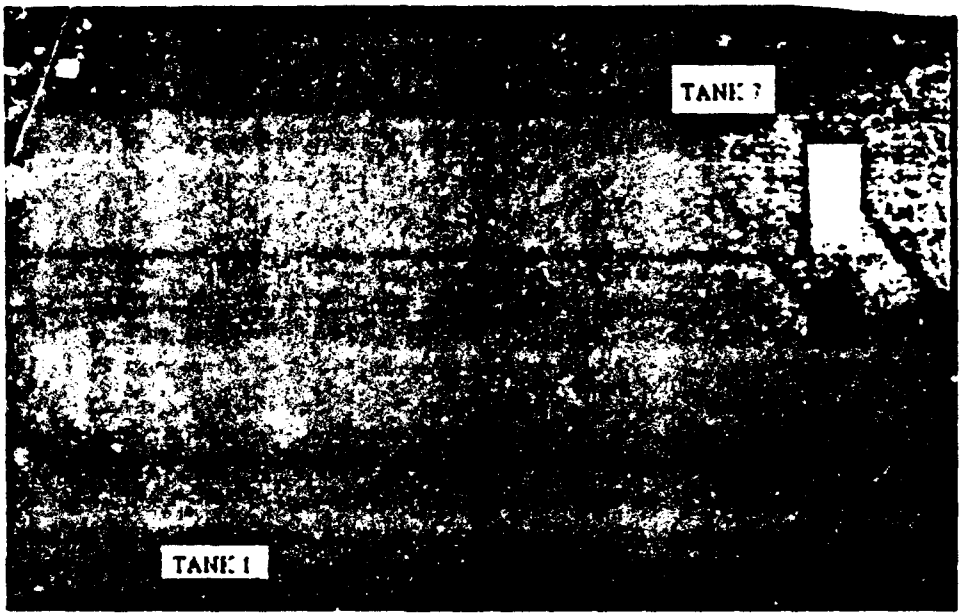

A. White Hot

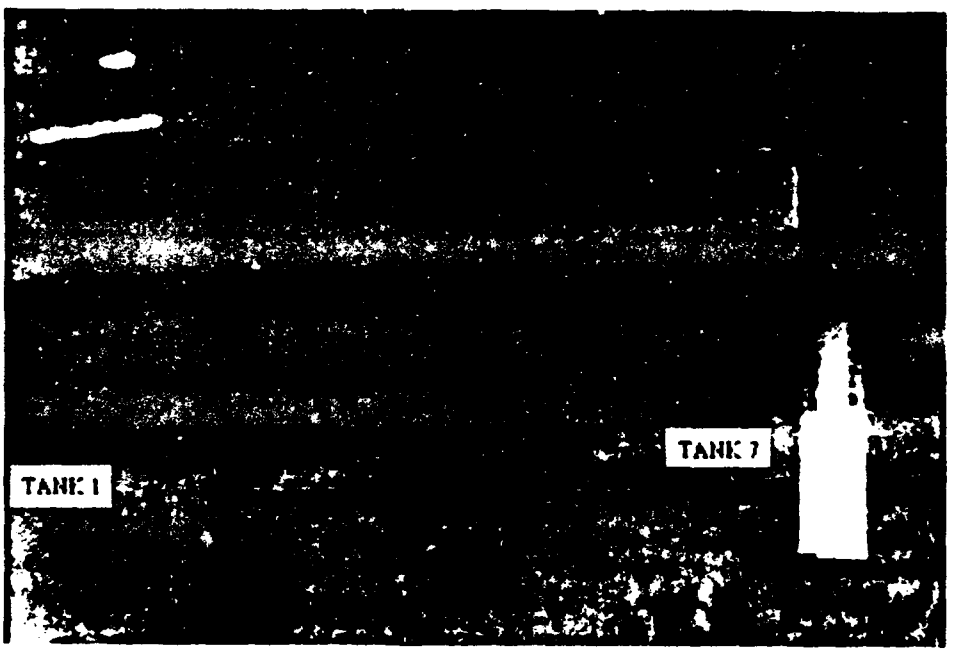

B. Black Hot

Figure 2-12. IRC 160ST, Nighttime, 4 May 1993, 1200 ft.

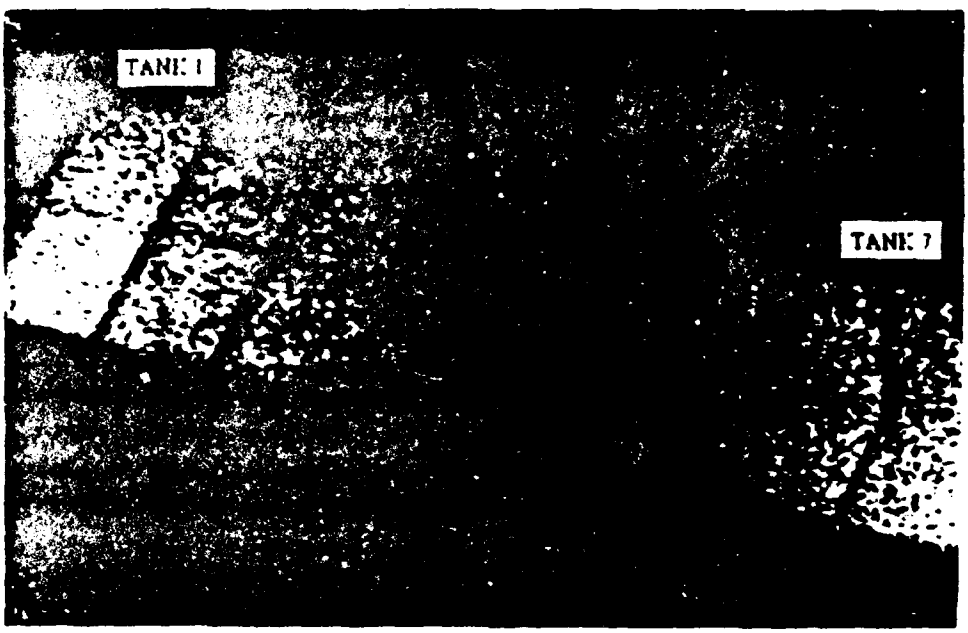

A. White Hot

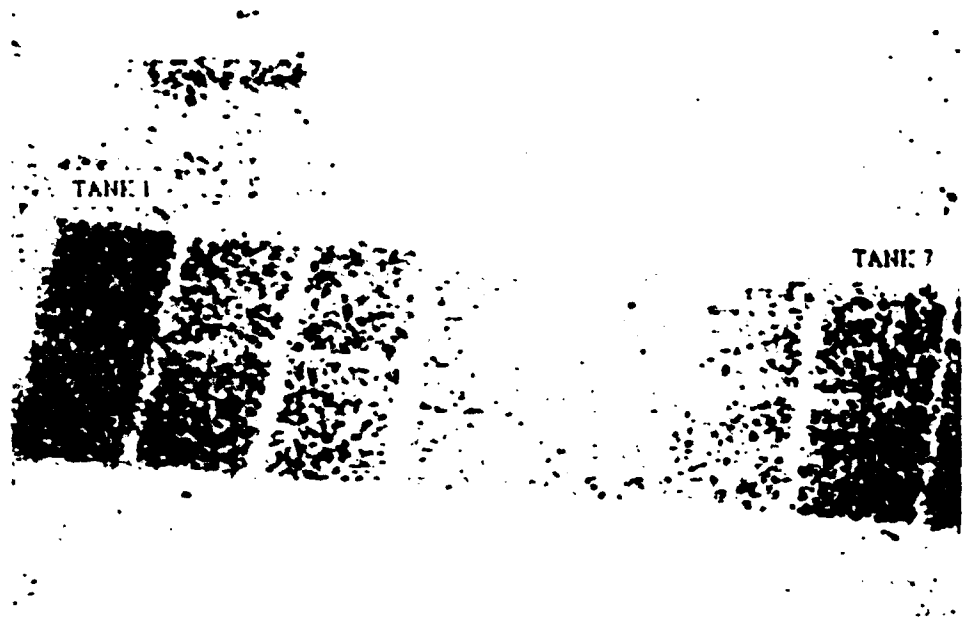

B. Black Hot

Figure 2-13. FSI Prism, Nighttime, 4 May 1993, 1200 ft.

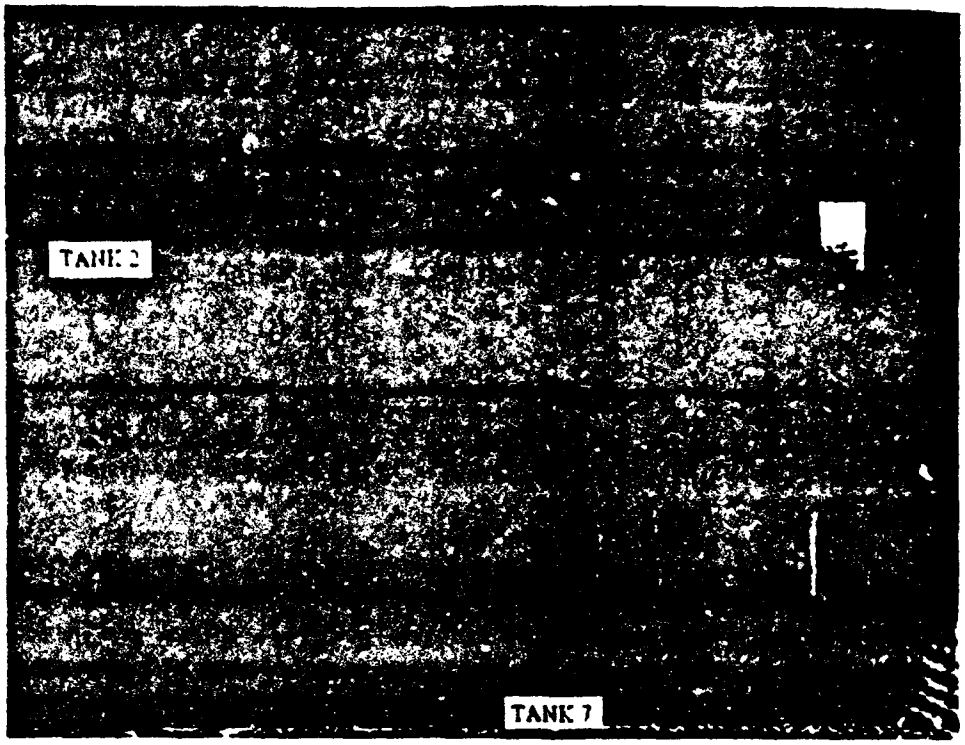

A. White Hot

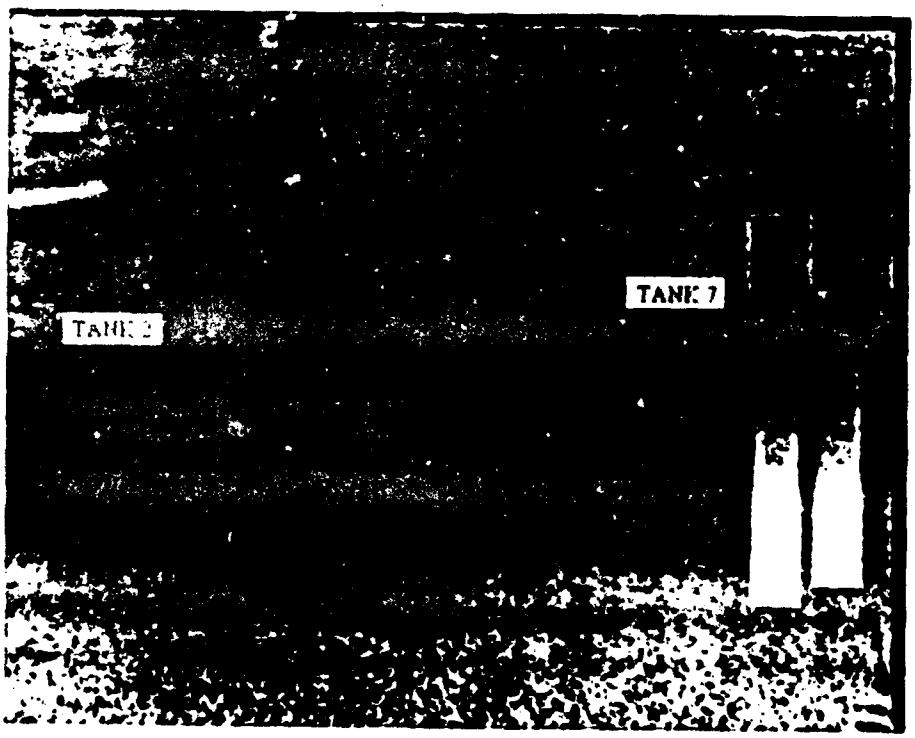

B. Black Hot

Figure 2-14. IRC 160ST, Nighttime, 5 May 1993, 1200 ft.

2.3 REPRESENTATIVE IMAGERY FROM INSTALLED LWIR SENSORS

Each of the LWIR sensors tested were installed as part of their respective aircrafts' avionics suite. The RS-18C provides a fixed FOV line scanning capability with IRLO, IRHI, and UV sensing options. The WF-360TL and FLIR 2000 are both LWIR sensors that permit the operator to switch polarity and FOV at will.

As will be illustrated below, each LWIR sensor consistently displayed the ability to detect oil on water both day and night.

2.3.1 Daytime LWIR Images

Figure 2-15 presents daytime FLIR 2000 imagery taken from 300 feet on 6 May. Frame "a" provides white = hot WFOV, frame "b" provides white = hot NFOV, and frame "c" provides black = hot NFOV.

Figure 2-16 presents daytime WF-360TL imagery taken from 500 feet on 6 May. Frame "a" provides white = hot WFOV, frame "b" provides white = hot NFOV, and frame "c" provides black = hot narrow FOV.

Figure 2-17 presents daytime imagery from the RS-18C on 6 May, 1993 at 500 ft. Frame "a" provides IRLO, frame "b" provides IRHI, and frame "c" provides UV images. These test tank images were extracted from much larger, full-swath line scanner images and are printed here without any reduction.

Discussion of Daytime LWIR Imagery

For the comparison of daytime LWIR and visible spectrum images, figure 2-3 frame "b" was taken at the same time as figure 2-16 frame "a" from the shared WF-360TL gimbal mount. The IR sensor had more difficulty detecting the lube oil in test tank cell 7 than the TV camera did, but it was better able to detect a faint sheen extending northward along the east berm of the northern cell of tank 2. The FLIR 2000 (figure 2-15) provides a capability similar to the WF-360TL. The RS-18C (figure 2-17) does show the oil in the southern section of the tanks, but because of the large scale display format, does not show much edge feature detail. The IRHI mode of this sensor, although quite sensitive to small temperature differences, has a relatively small dynamic range and during daytime searches provided relatively poor oil/water contrast. The IRLO channel, although less sensitive to small apparent temperature differences, provided excellent contrast between the sun-warmed oil and the relatively cool water.

A. White = Hot, Wide Field of View

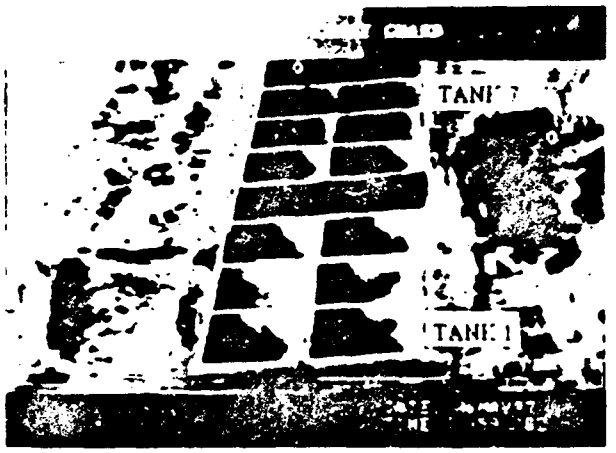

B. White = Hot, Narrow Field of View

C. Black = Hot, Narrow Field of View

Figure 2-15. FLIR 2000, Daytime, 6 May, 1993, 300 ft.

A. White = Hot, Wide Field of View

B. White = Hot, Narrow Field of View

C. Black = Hot, Narrow Field of View

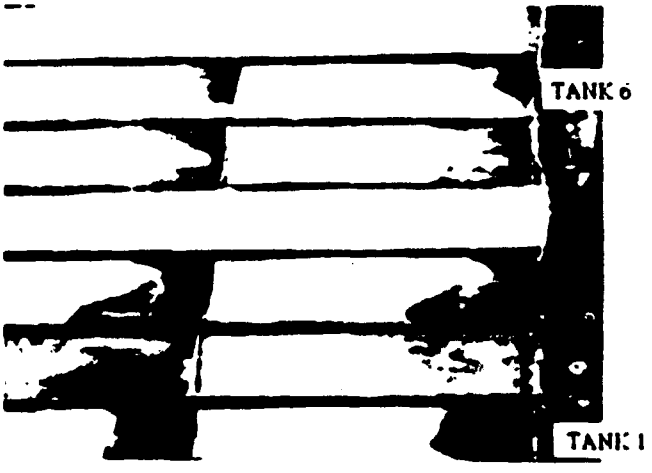

Figure 2-16. WF-360TL, Daytime, 6 May, 1993, 500 ft.

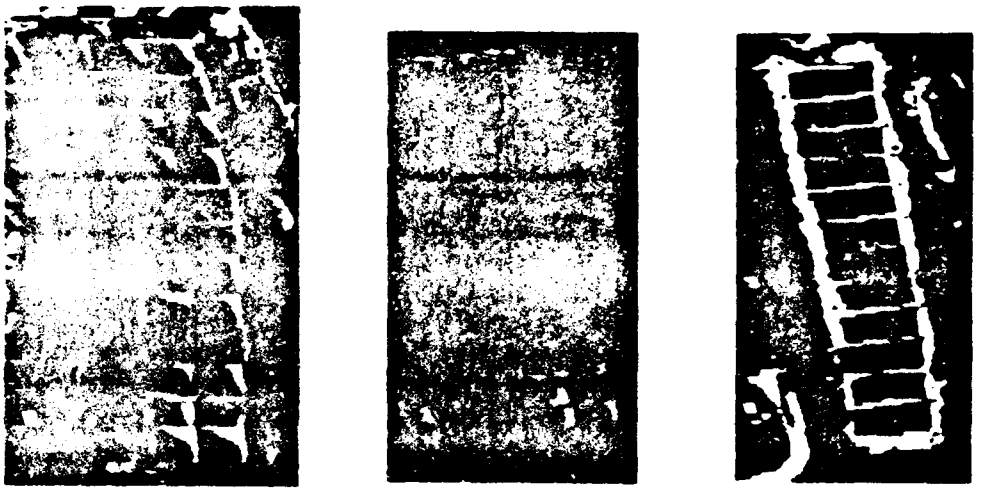

A. IRLO Image B. IRHI Image C. UV Image

Figure 2-17. RS-18C, Daytime, 6 May, 1993, 500 ft.
(tank 1 at the bottom of all three images)

The FLIR 2000 and WF-360TL provided the ability to observe fine detail in the slicks where sufficient oil/water contrast existed. The scale of the images provided by the RS-18C is too large to be useful in this evaluation. Even at 500 ft., which is typically the lowest practical altitude for searches with this sensor, image detail is insufficient for comparison to the FLIR sensors. Frames "b" and "c" from both figures 2-15 and 2-16 demonstrate the exceptional ability of these FLIR sensors to capture edge detail with NFOV. The daytime temperature differences between oil and water provide better information about the relative oil thickness and area coverage than is possible with the visible spectrum images. An altitude of 1200 ft. reduced the test tank to a size such that slick details were lost by both FLIRs when operated in wide FOV.

Both FLIR sensors provided clear images. Although the portable video recording system installed to capture WF-360TL test imagery quite often contained noise caused by the aircraft power supply, the air crew assured observers that this noise is not present on the aircraft's permanently-installed recorder. The FLIR 2000 NFOV displayed an annoying jitter caused by airframe-induced camera vibrations. When this motion (which occurred at lower aircraft speeds) was present, images were very blurry; when absent, images were very clear.

Just as with the MWIR sensors, video polarity does not appear to affect image quality or the ability to obtain a clear image. Although black = hot or white = hot polarities are able to present the same quality image, some operators will find it easier to consistently obtain a clear image in one polarity simply because of their individual interpretations of visual cues. Switching from one polarity to the other does not appear to provide any advantage when attempting to obtain a clearer image.

2.3.2 Nighttime LWIR Images

Figure 2-18 presents nighttime RS-18C imagery taken from 1000 feet on 5 May. Frame "a" provides IRLO and frame "b" provides IRHI images.

Figure 2-19 presents nighttime FLIR 2000 imagery taken from 1200 feet on 5 May. Frame "a" provides white = hot WFOV, frame "b" provides white = hot NFOV, and frame "c" provides black = hot NFOV.

Figure 2-20 presents nighttime WF-360TL imagery taken from 1000 feet on 5 May. Frame "a" provides white = hot WFOV, frame "b" provides white = hot NFOV, and frame "c" provides black = hot NFOV.

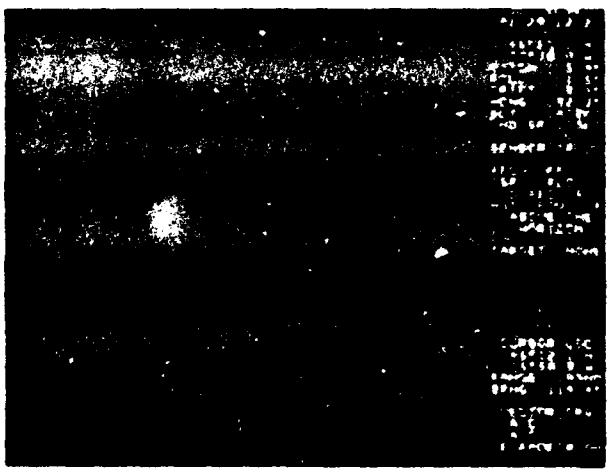

A. IRLO Image

B. IRHI Image

Figure 2-18. RS-18C, Nighttime, 5 May, 1993, 1000 ft.

A. White Hot, Wide Field of View

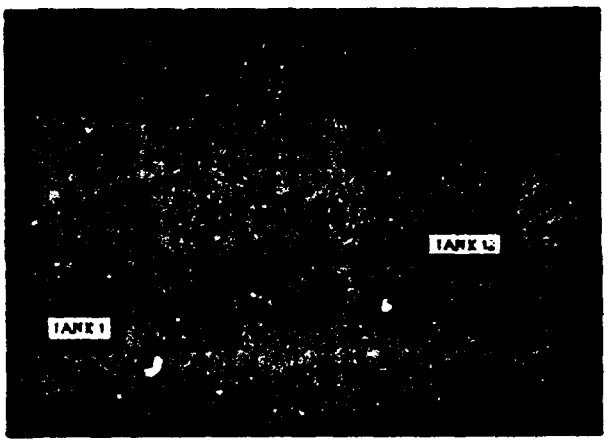

B. White Hot, Narrow Field of View

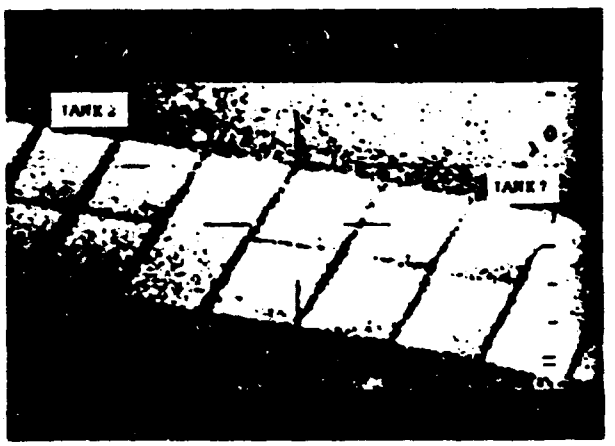

C. Black Hot, Narrow Field of View

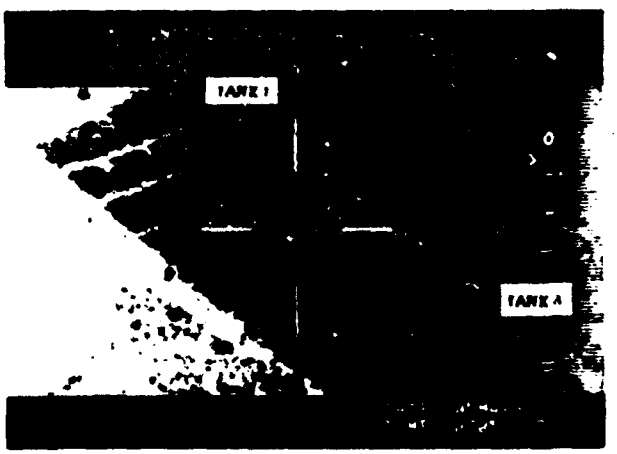

Figure 2-19. FLIR 2000, Nighttime, 5 May, 1993, 1200 ft.

A. White Hot, Wide Field of View

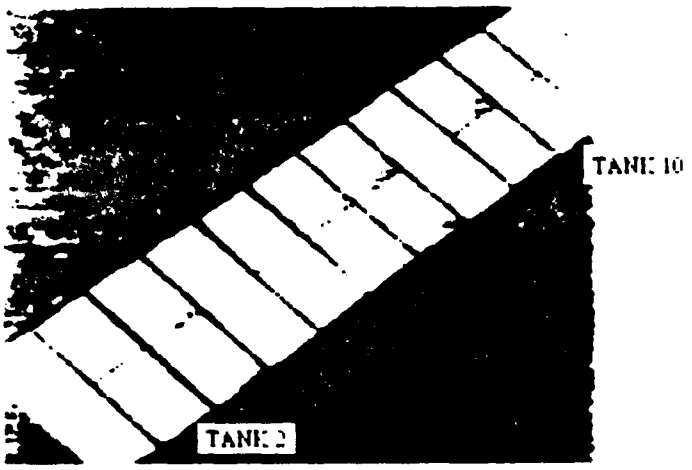

B. White Hot, Narrow Field of View

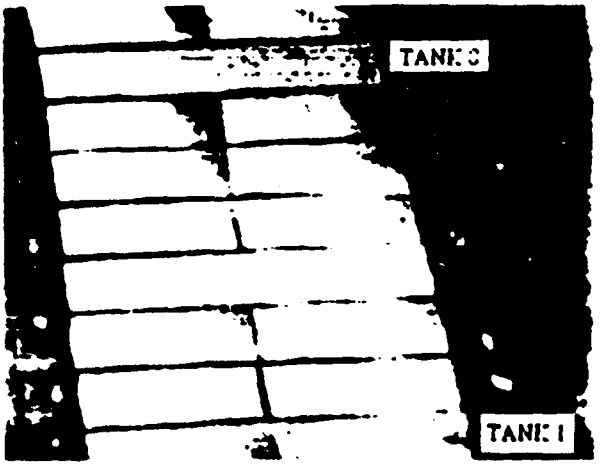

C. Black Hot, Narrow Field of View

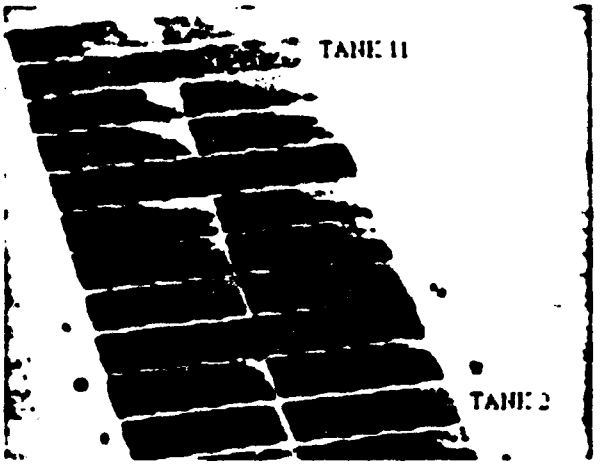

Figure 2-20. WF 360TL, Nighttime, 5 May, 1993, 1000 ft.

Discussion of Nighttime LWIR Imagery

Nighttime imaging of the test tanks is where the LWIR FLIR imagers proved most advantageous over the other sensors. These sensors were able to detect the oil/water contrast on both nights and even at the higher altitudes, the NFOV often provided image detail permitting identification of the oil slick boundaries and an indication of the relative thicknesses of different areas within the slicks. At night from 1200 ft., the FLIR 2000 WFOV did not provide sufficient image resolution to detect the oil; however, the NFOV provided good contrast and edge definition.

2.4 ERGONOMICS

Ergonomic considerations discussed in this section are based upon comments written on the data logs, verbal comments captured on the audio portion of the S-VHS tapes, and post experiment comments from data recorders.

There was no audio track on either the HU-25B or the HU-25C aircraft tapes, so operator comments concerning the RS-18C and WF-360TL are limited to those written on data recorder sheets. Since these sensors have standard installations and have been in regular service, most ergonomics problems have been addressed. The major system design issue identified relative to the installed sensors is jitter that was present in some FLIR 2000 imagery. This image jitter, caused by uncompensated helicopter vibrations at low airspeeds (below 50 kts), can cause fatigue in an operator concentrating on the screen image. Crew comments concerning this most often included discussion of fatigue and motion sickness.

The hand held units were much less familiar to the operators, and on each successive day of use, the ability of the sensor operators to properly tune the test tank image improved. Throughout the experiment, operators of the hand-held units experienced trouble with tuning and focus controls. Many times when an operator first used a sensor the imagery was seldom usable, and even after operators became more familiar with the sensors a slip of the finger could drastically reduce image quality. Figure 2-21 best illustrates this problem. The operator was tuning the test tank image shown in frame "a" on the Agema 210. Frame "b" was taken seconds later after the operator accidentally depressed the "increase contrast" button. In this case, it took more than 60 seconds before the image was properly retuned. The sequence shown in

figure 2-21 occurred during the day on 6 May when excellent oil/water contrast was available in the scene. In lower-contrast situations at night, operators experienced considerable difficulty locating and properly adjusting the correct controls to acquire properly tuned test tank images. On the night of 5 May, an operator with the IRC-160ST lost the picture to complete grey and had such difficulty re-acquiring the image that a discussion ensued as to whether any further attempts at imaging with the sensor should be made. The image was eventually re-acquired by alternating each control through extremes. This suggests that automated tuning with operator fine-tuning could be a useful feature to implement on these hand-held sensors.

Night searches during this field test provided ample demonstration of how a lack of sensor familiarity can hinder image acquisition. When using the hand-held sensors, inexperienced operators often lowered the instruments to their laps to locate desired adjustment controls and then had to relocate the test tanks while attempting to tune the image. When an inadvertent change in sensor settings occurred while the sensor was away from the operator's eye, quite often a significant amount of time was spent re-acquiring the image.

Another difficulty encountered during the test was the number of system components to keep track of and the conditions under which the hand-held units were being operated. Each imager was connected to a separate battery system and to the video recorder. In addition to the imager connections, the video recorder was connected to an audio patch and an external video monitor. Because the operators of the hand-held imagers were not air crew personnel, each had an unfamiliar helmet and microphone and had to adjust to the airborne environment. Maintaining awareness of each of these equipment pieces while strapped in the flight mechanic's chair in the open helicopter door made operating these units very difficult at times. Simplifying cabling, consolidating components, and providing an automated coarse contrast/tune function to quickly adjust for ambient conditions could reduce the level of distraction to the operator while improving safety and mission effectiveness.

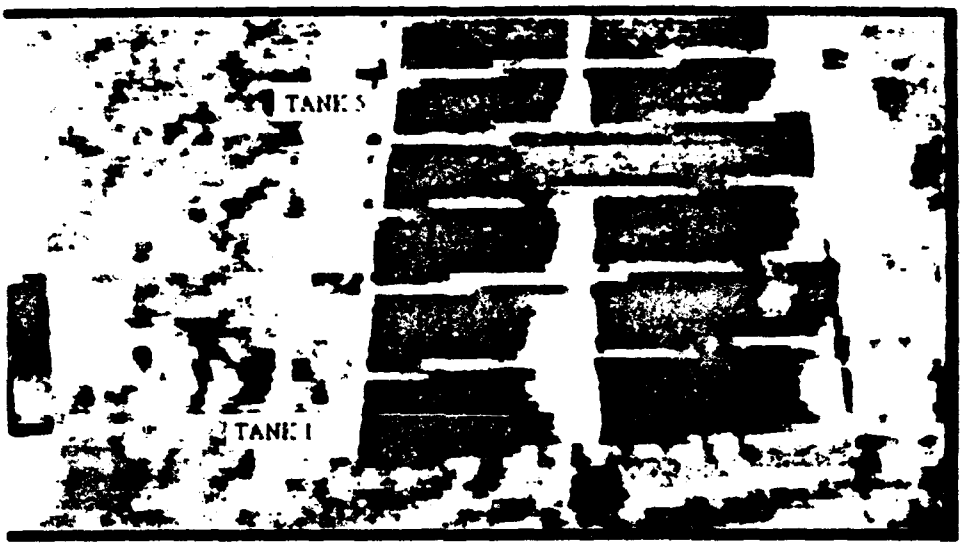

A. Image well tuned and slightly out of focus

B. Image after contrast control bumped

Figure 2-21. Agema 210, Day, 6 May 1993, 300 ft.

2.5 SELECTION OF IMAGERY FOR DETAILED ANALYSIS

Based on the available image data set reviewed in this chapter, several analysis topics of interest were developed and are discussed in chapter 3. These topics include:

- LWIR versus MWIR capabilities,
- Effects of incidence angle,
- Effects of daytime specular reflection on IR imagery,
- Effect of altitude and field of view on scene content and detail.

Imagery to support these analyses will primarily be from the IRC-160ST, FLIR 2000, and WF-360TL. These sensors have the broadest representation within the data set relative to environmental conditions, viewing angle, altitudes, and available image detail.

Section 3.4 will present an estimation of oil thickness using selected images.

CHAPTER 3
IMAGE ANALYSIS

Chapter 2 introduced imagery from each sensor used for this evaluation. It summarized the ability of the imagers to provide clear detail under various conditions. Among the imagery available, the IRC-160ST, FLIR 2000, and WF-360TL supplied the clearest and most complete set of images. Images from these sensors will be used for the analyses presented in this chapter.

Section 3.1 compares the strengths and weaknesses of the MWIR and LWIR sensors. A side-by-side comparison of night time imagery from the IRC-160ST and FLIR 2000 is presented. Section 3.2 discusses the effects of incidence angle on the ability of the sensors to detect oil on water in daytime and nighttime missions. Section 3.3 discusses the effects of solar heating and specular reflection on the IR imagery. Section 3.4 presents a discussion of the effects of altitude and field of view on image content and quality. Section 3.5 will evaluate the accuracy with which the extent of the oiled area was depicted by the infrared sensors. This will be done by comparing oil thickness calculations made using surface truth data with thickness estimates made using apparent slick areas (from the IR images) and the known quantities of oil in the test tanks.

3.1 COMPARISON OF MWIR AND LWIR SENSOR IMAGES

When visibility is good, daytime visible-spectrum imagery contains sufficient information to detect and characterize oil slicks. However, as discussed in chapter 1 the ability to obtain detailed, nighttime visible spectrum images is severely limited. Since IR offers the most potential for improved operating capabilities at night, this comparison of MWIR and LWIR sensors focuses on their nighttime imaging performance.

Figures 3-1, and 3-2 provide night imagery for 4 and 5 May, 1993. In figure 3-1, frames "a" and "b" are from the night of 4 May and provide images from the IRC-160ST (MWIR; 3-5 micron wavelengths) and FLIR 2000 (LWIR; 8-12 micron wavelengths), respectively. In figure 3-2, a similar image pair is shown from the night of 5 May. Each of these images is white = hot video polarity taken from south of the test bed at 1200 foot altitude. FLIR 2000 narrow field of view images were chosen for this comparison because they provide a FOV that is similar to that provided by the fixed-lens IRC-160ST.

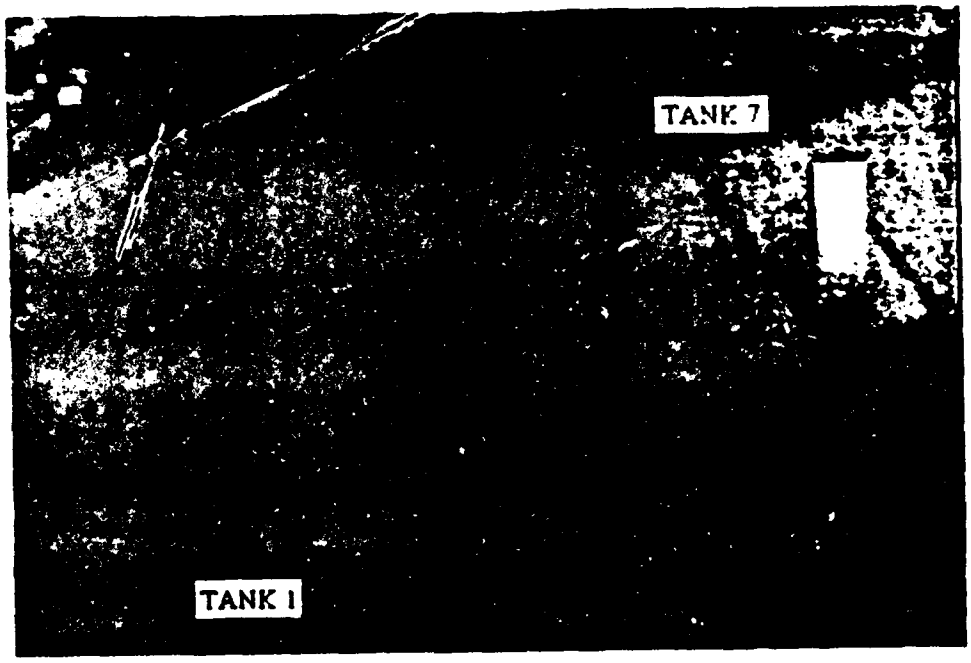

A. IRC-160ST, White Hot

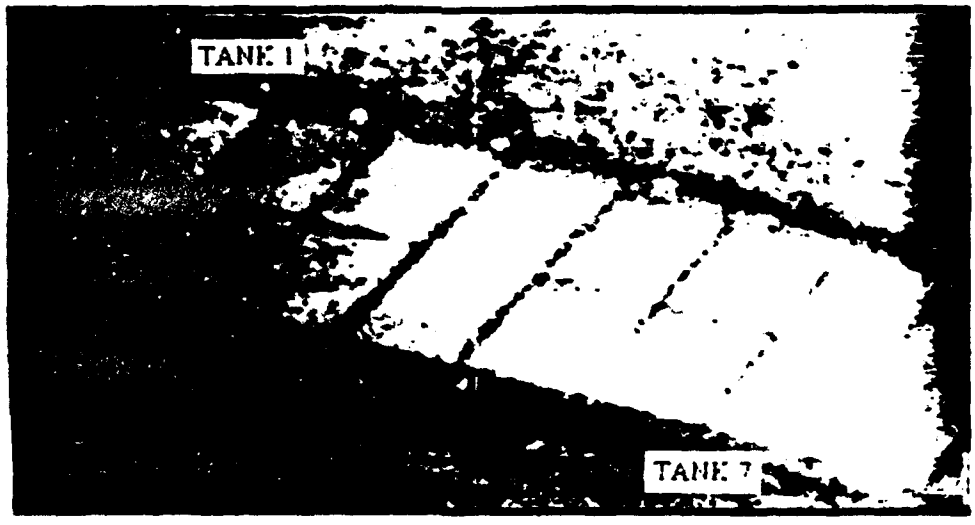

B. FLIR 2000, White Hot, Narrow -FOV

Figure 3-1. Comparative Imagery, Night, 4 May 1993, 1200'

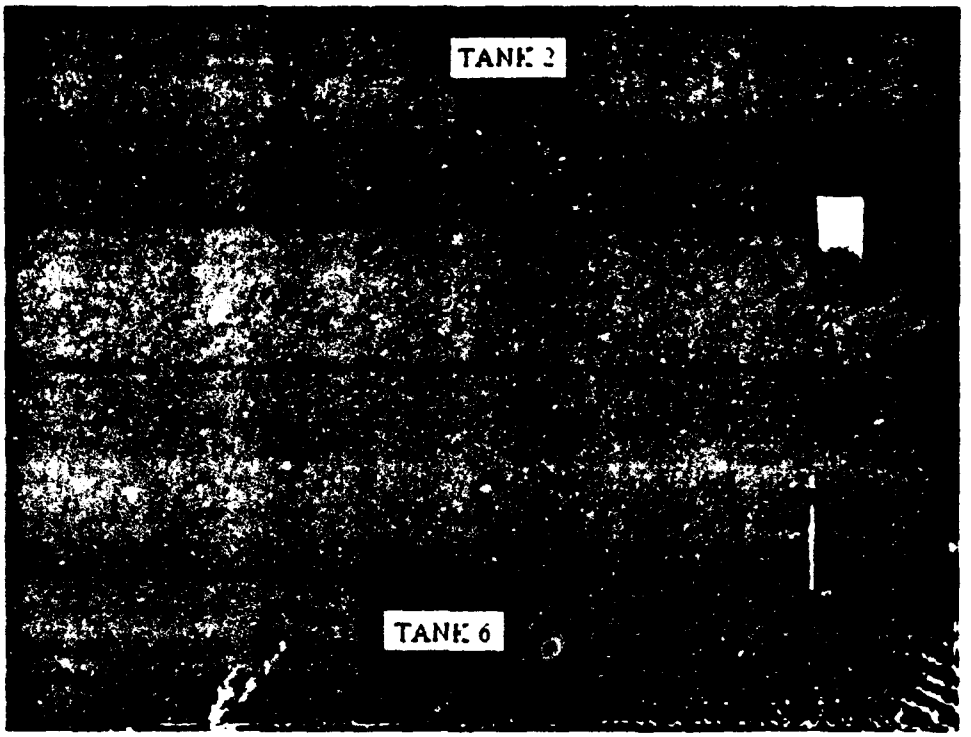

A. IRC-160ST White Hot

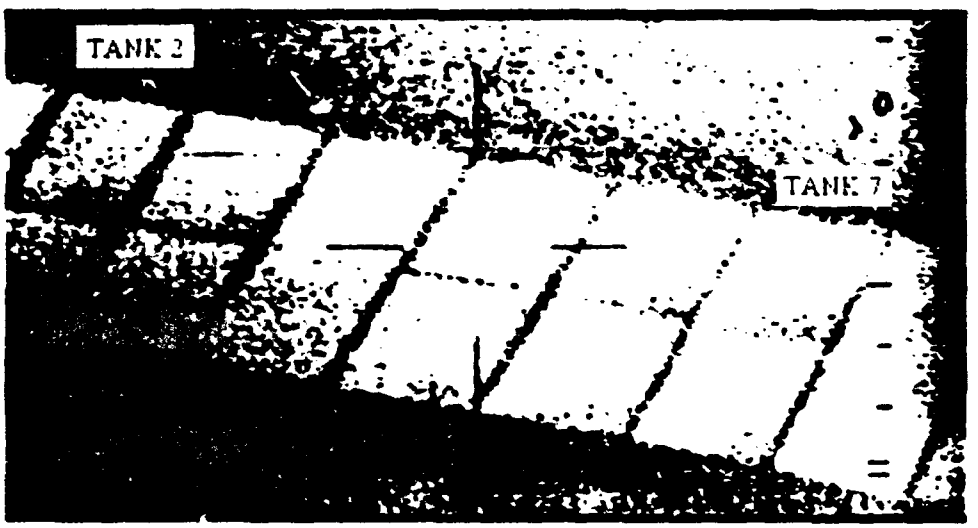

B. FLIR 2000, White Hot, Narrow-FOV

Figure 3-2. Comparative Imagery, Night, 5 May 1993, 1200'

In frame "a" of figure 3-1, the sand berms are plainly seen and in focus, the 8 oil drums standing along the western half of the test tank sides are visible, but there is minimal oil/water contrast in the MWIR image. Tank 5, which contains Terra Nova oil, has the most visible oil in this image, and even that is minimally detectable with knowledge of where the oil is.

Figure 3-1, frame "b" provides the same detail of physical features; however, the thermal contrast in the LWIR image provides a sharper picture and displays the oil/water boundaries in the individual tanks.

As with figure 3-1, frames "a" and "b" of figure 3-2 clearly show the physical properties of the test area. Figure 3-2 frame "a" shows that the MWIR oil/water contrast was better on the night of 5 May. The location of the oil can be ascertained without prior knowledge on the part of the observer. The reader may note that the FLIR 2000 image in figure 3-2, frame "b" is much grainier than the one in figure 3-1, frame "b". This appears to be due to a slight maladjustment of the FLIR 2000 contrast control. The LWIR sensor still provides better oil/water contrast than the MWIR sensor.

In attempting to identify a reason for the mixed nighttime results obtained with the MWIR sensor, it is useful to compare the environmental conditions for the nighttime sorties. From tables 1-4 and 1-5, the difference between the water temperature in the test tanks and the recorded air temperatures was greater on the night of 5 May than on the night of 4 May. On the night of 5 May, the average difference between air and water temperatures was 4.0°C while on the night of 4 May the average difference was 0.4°C. (It must be noted that the tank temperatures were taken once during each sortie, and the air temperatures varied throughout the sortie.) The relative humidity was 83 percent on 5 May and 68 percent on 4 May.

Given the above environmental data, the differences in MWIR oil/water contrast between figures 3-1a and 3-2a can be loosely associated with differences in the temperature and humidity conditions under which they were obtained. Figure 3-1 indicates that the LWIR sensor was able to depict oil/water contrast on 4 May when environmental conditions were not conducive to detection by the MWIR sensor. In the warmer, more humid conditions of 5 May (figure 3-2), the MWIR sensor was able to detect the oil/water contrast.

The discussion above illustrates that, at night, the LWIR sensors benefited from stronger and more consistent oil/water contrast signatures. This reduced the LWIR sensors' susceptibility to small changes in environmental conditions and resulted in more reliable oil slick detection than achieved with MWIR sensors. Reference 3 will demonstrate that these observations were consistent with IR theory.

3.2 INVESTIGATION OF INCIDENCE ANGLE

The influence of incidence angle on oil slick detection performances was evident only in isolated cases during the Petawawa test. The effect of incidence angle will be illustrated using daytime IR imagery taken from the WF-360TL, which has the advantage that simultaneous TV imagery was recorded. Figures 3-3 and 3-4 provide white = hot and black = hot, WFOV images, respectively, taken at an altitude of 1000' during the day on 5 May. Each figure presents the IR image at the top and a simultaneous TV image on the bottom. The white = hot image is taken approximately 5 minutes earlier than the black = hot image.

In this set of images, both polarities provide similar detail; however, the black = hot image appears to provide a better representation of the lube oil in tanks 2 and 7. In order to understand why this occurred, the dynamic nature of the target scene must be described. As discussed in chapter 1, the lube oil absorbs less solar energy and is therefore less emissive than the black crude oils when exposed to sunlight. This results in a weaker heat signature for lube oil in the infrared images. Between the times the white = hot and black = hot images were taken, the wind (0-2 knots) was shifting from a westerly to a more southerly direction. The lube oil was spread thinly across tanks 2 and 7 when the white = hot image was taken, after which it began to concentrate along the northern edge of the tank. This movement of the oil is confirmed in the TV images provided. The lube oil was more easily detected 5 minutes later during the black = hot pass when the slightly-warm oil was more concentrated.

The subtle influence of incidence angle on oil slick detection performance is illustrated in figure 3-5. In this image, the thinly-spread lube oil in tanks 2 and 7 was not detected. This image was taken approximately 5 seconds earlier than the images in figure 3-3 and during the same pass over the test tank. This pair of images demonstrates that in a marginal daytime contrast situation, a low incidence angle (below approximately 40 degrees) provides a weaker signal at the sensor than a higher incidence angle. During the pass represented in figure 3-4, the oil is concentrated closer to the oil berm, and the thermal signature is strong enough that incidence angle does not significantly affect the ability to detect the oil slick.

Reference 3 will present theoretical data that suggest that, at night, incidence angle may actually have the opposite influence on oil slick detection. This implies that in marginal nighttime viewing conditions, lower incidence angles (low altitude/moderate range) may provide better oil/water contrast than steep depression angles. This influence could not be identified in any of the nighttime imagery collected during the Petawawa test.

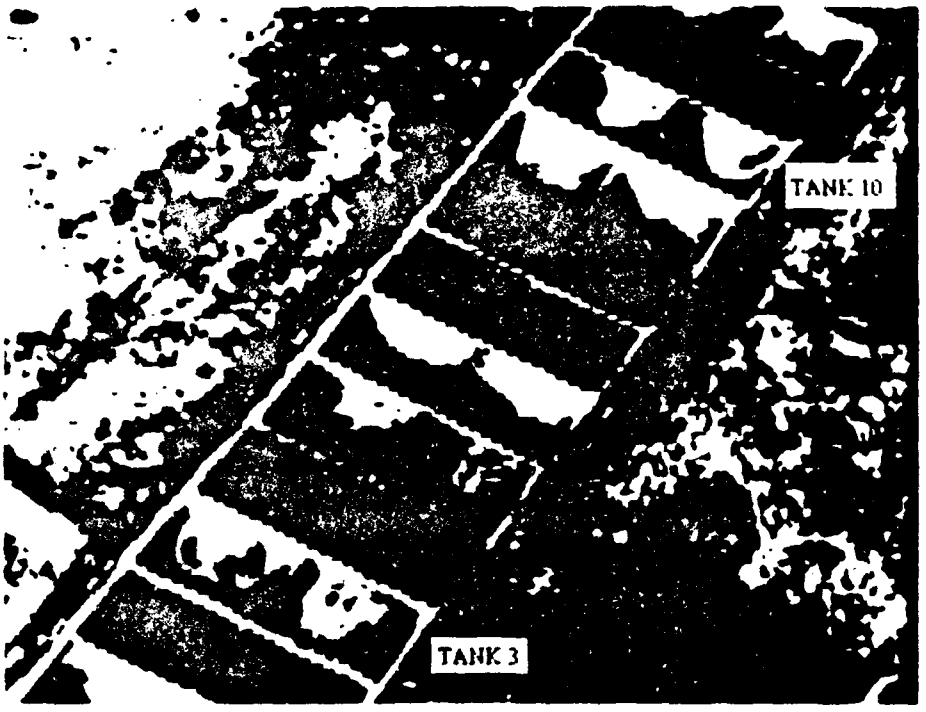

a. IR Band, Wide Field of View

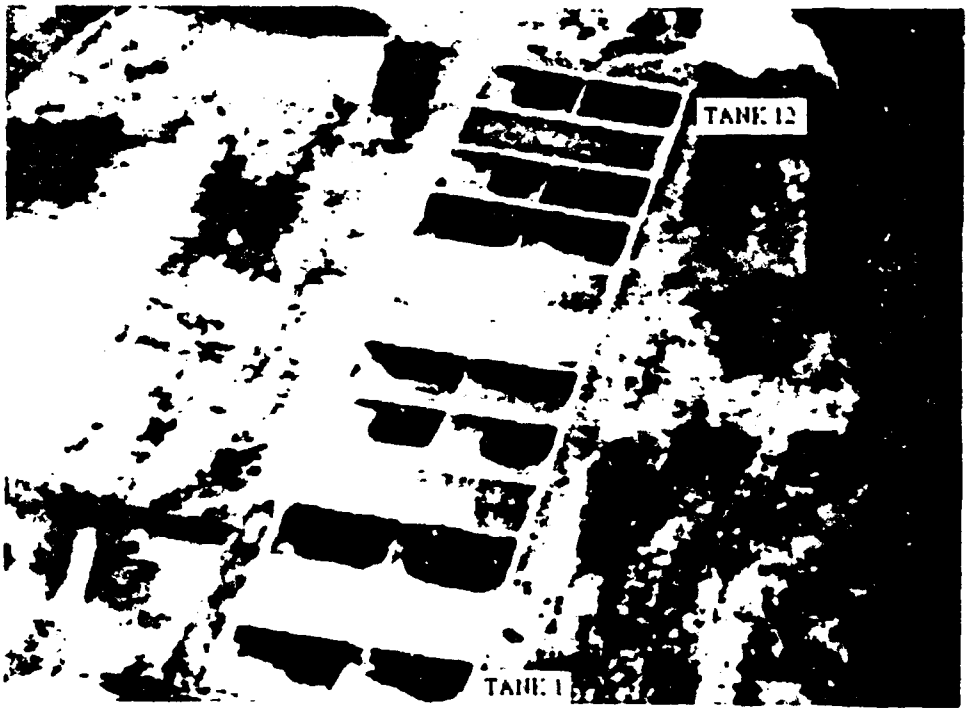

b. Visible Band, TV Camera

Figure 3-3. WF-360TL, Day, 5 May 1993, 1000 ft., White Hot Pass

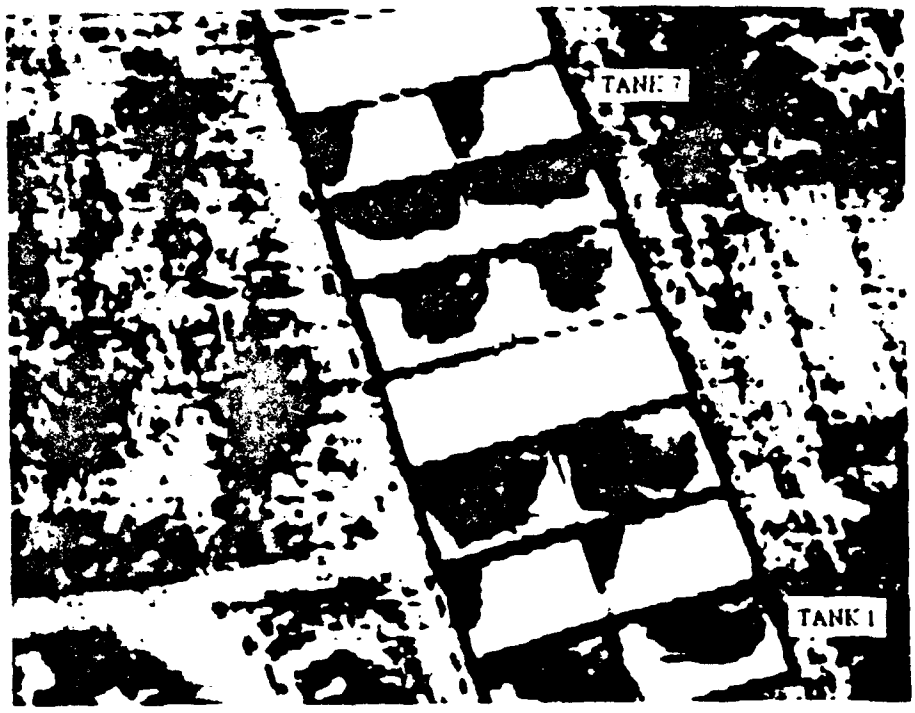

a. IR Band, Wide Field of View

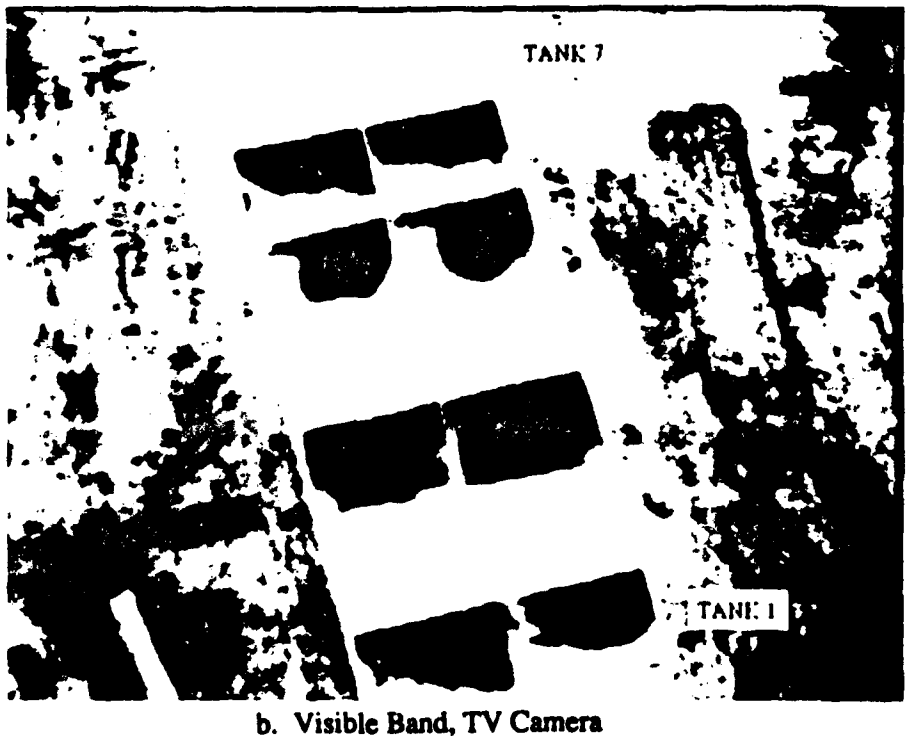

b. Visible Band, TV Camera

Figure 3-4. WF-360TL, Day, 5 May 1993, 1000 ft., Black Hot Pass

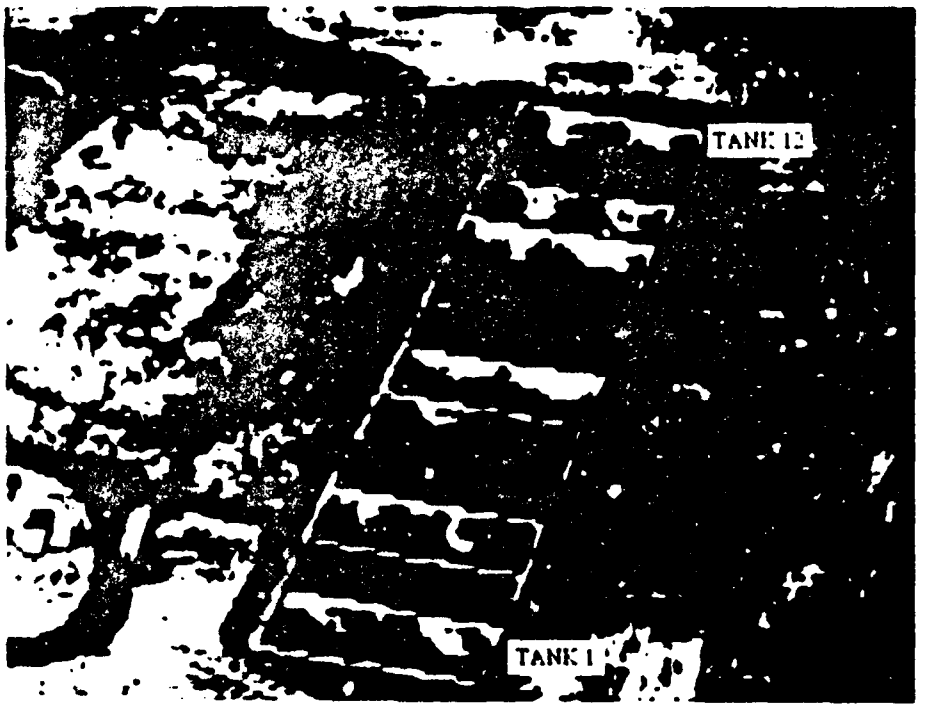

Figure 3-5. WF-360TL, Day, 5 May 1993, 1000 ft.
(off nadir view)

3.3 MWIR SPECULAR REFLECTION

Visible specular reflection occurs when energy from a light source, such as the sun, bounces off a surface being viewed in a mirror-like fashion. It is typically a hindrance only when looking directly towards the reflecting surface. The same phenomenon can occur in infrared images. In some of the nighttime IR imagery reviewed, the heat reflection of people in the scene is visible on the surface of the test tank water (see, for example, figure 2-8 "b"). This is a form of reflection that is not likely to hinder sensor performance since it covers only a small area. At night few heat sources would be expected to hinder oil slick observation (vegetation along riverbanks is an example).

A more significant source of thermal specular reflection comes from the sun at MWIR wavelengths. The problem of daytime specular reflection at MWIR wavelengths is demonstrated in figure 3-6. This image was taken looking west with the sun located southwest of the test area. Small wind-induced capillary waves on the water's surface are reflecting MWIR solar energy to the sensor, hindering the viewer's ability to detect the oil slicks. There is very little solar energy available at LWIR wavelengths, and therefore LWIR sensors are not as susceptible to this problem.

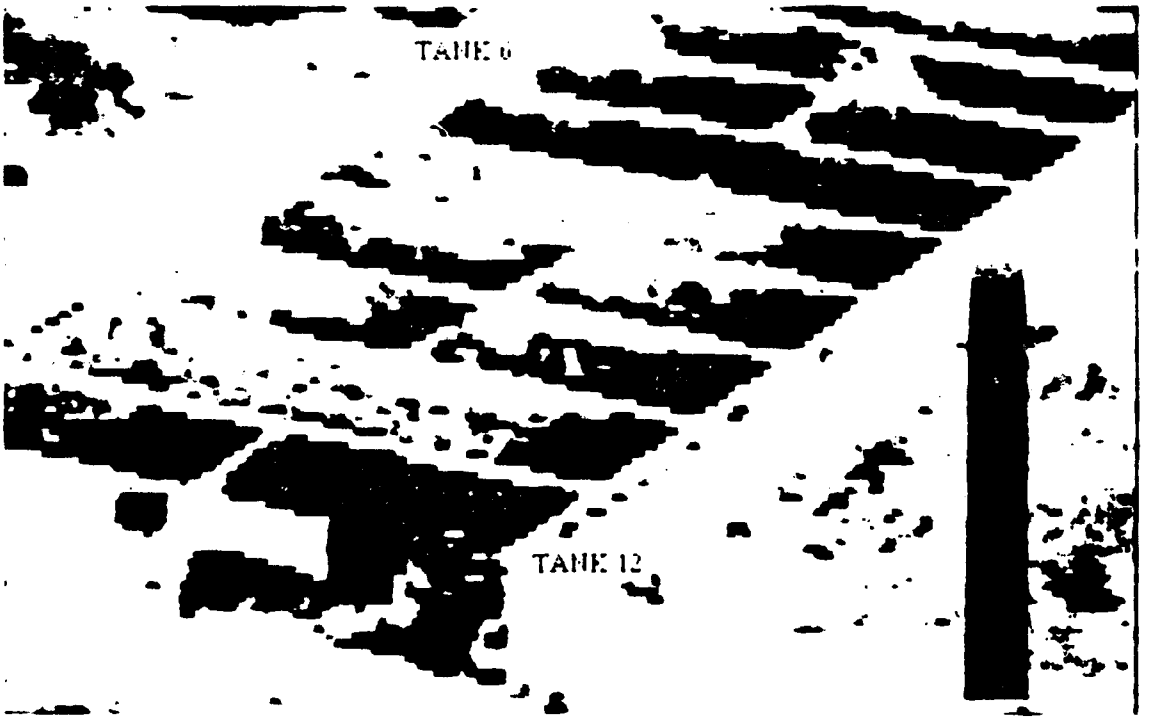

Figure 3-6. IRC-160ST Image Showing Specular Reflection

3.4 ALTITUDE AND FIELD OF VIEW

3.4.1 MWIR Altitude and Field of View

The fixed lens design of the hand-held sensors limits the ability of an operator to change the FOV. FOV size can be altered by changing the distance to the target, or for the FSI Prism and IRC 160ST, by manually swapping the lens. Figure 3-7 presents an example of how altitude can affect FOV and, in the process, image detail when sufficient contrast exists to provide an oil/water boundary. While the higher-altitude image provides information over a greater area, the lower altitudes permit viewing finer detail within the view available. At 300 feet, oil/water boundary detail and differences between sheen areas and thicker portions of the oil slick are visible while at 1200 feet, the image only depicts areas of contrast. In this set of images, the 500-foot altitude provides a useful compromise, depicting a significant portion of the test tank while maintaining some of the contrast differences seen in the 300-foot altitude image. The operational lesson demonstrated by this series of images is that, while a wider FOV may be adequate for detecting thermal anomalies in a wide-area scene, lower altitudes or longer lenses are required to observe slick edge detail and thermal gradients which might help to confirm that an anomaly is an oil slick.

3.4.2 LWIR Altitude and Field of View

While images obtained from the LWIR sensors exhibit properties similar to those seen in the MWIR images, the ability to switch from WFOV to NFOV at will gives the installed systems a significant advantage over a fixed lens sensor. Investigation of scene detail becomes a matter of selecting a region of interest and switching the lens. The speed of the HU-25C reduces the benefit of NFOV below 1000 ft because the image changes too quickly to permit an operator to distinguish and study scene features in real time.

A. 1200 ft.

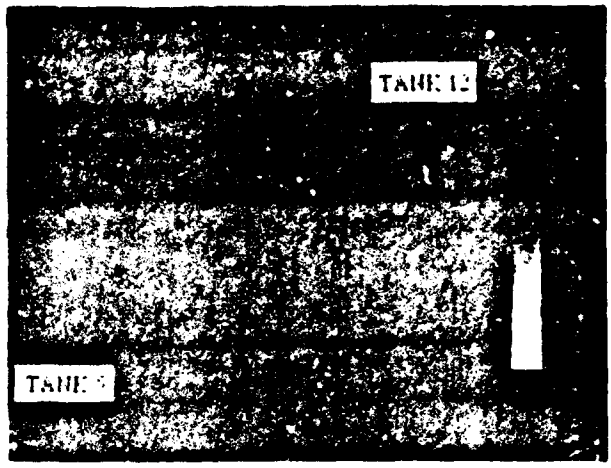

B. 500 ft.

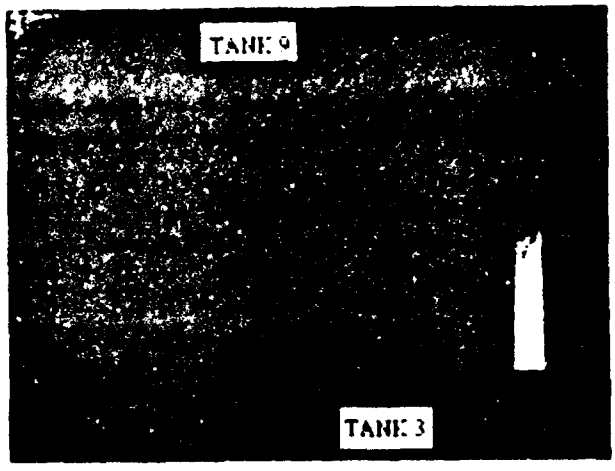

C. 300 ft.

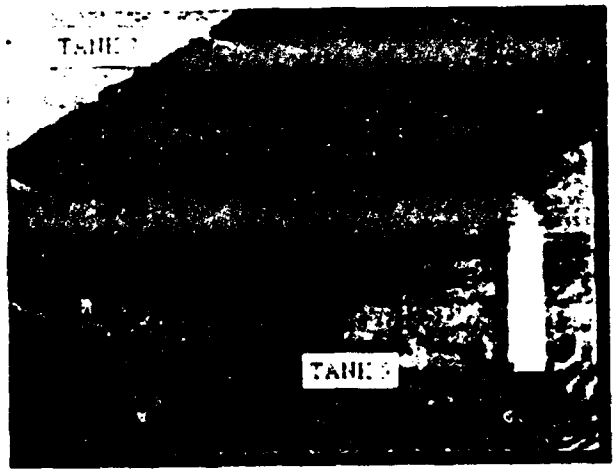

Figure 3-7. IRC-160ST, Black = Hot, Night, 5 May, 1993, Altitude Comparison. (50mm lens)

3.5 OIL SLICK AREA AND THICKNESS ESTIMATES

Table 3-1 provides "snapshot" oil thickness estimates derived from 5 May surface truth and IR image data. Oil thickness estimates have been developed and are presented below solely as a measure of the IR sensors' ability to depict areas of relatively thick oil within the slicks. No operational method currently exists to consistently and accurately measure oil thickness through the use of remote sensing. The oil does not maintain a uniform thickness throughout a slick, and variable wind, as experienced during this experiment, can rapidly change the dimensions and position of a slick. The surface "truth" thickness estimates obtained by Environment Canada were made at least 2 hours prior to the Coast Guard flights. They are provided here as same-day reference estimates of oil thickness and should not be expected to agree precisely with the values derived from the IR images.

The three methods Environment Canada ground personnel used to estimate oil thickness were: oil/water sample collection by bailer; oil/water sample collection with sorbent pads; and measurement of the oil slick physical dimensions. In the third method, the physical dimensions of the oil slick in each test tank cell were determined using a tape measure. Oil slick thickness was computed by dividing the slick area by the known volume of oil. Table 3-1 includes oil slick thickness estimates generated from the physical dimension measurements.

The daytime IRC-160ST and FLIR 2000 thickness estimates were calculated using near time-coincident images taken from the HH-60J helicopter. The daytime WF-360TL IR and TV images used are time-coincident and were obtained approximately 15 minutes later than the helicopter images. The oiled regions of the tanks were located in the northeast corner during the helicopter overflights, and in the east and southeast corners during the HU-25C (WF-360TL) overflights. The nighttime images used to estimate oil thickness are all approximately time-coincident, and show the oil slicks in essentially the same locations.

Area calculations were made using EarthView 4.0, an image analysis software package. This software provides the ability to bound a region and calculate the area within the boundary. Figure 3-8 demonstrates this procedure for tank 7 using a night image taken from the WF-360TL. The thin white line bounds the oiled region where the oil slick area measurement was taken. The thicker white line bounds the total tank area, which was also measured. Multiplying the ratio of these two area measurements by the known true area of the test tank yielded the actual surface area of the oiled region. Dividing the known volume of oil that had been added to the tank by the surface area yielded a thickness estimate.

The area measurements did not include sheen oil when it could be identified as such in the IR images because the sheen contains such a small amount of oil. Where the IR images depicted variable grey levels within the oil slick, no effort was made to quantify the variability of the oil thickness. In table 3-1, where no thickness data is present, the images selected for the area comparison did not include a sufficient portion of the tank or oil to make area measurements possible. This occurred when a significant portion of the test tank was out of view in the image.

The data in table 3-1 confirm that, during the day, the IR imagers were able to depict oil slick boundaries accurately enough to provide area/thickness estimates that were consistent with those determined using ground-based measurements. It is important to note, however, that without knowing the volume of oil in the test tanks, oil slick thickness could not be determined from the IR images. Indeed, even the sorbent pad and bailer sampling methods used by Environment Canada yielded inconclusive results. Variation in the thickness estimates obtained from night IR images suggest that the they may not have always depicted the entire oil slick surface area.

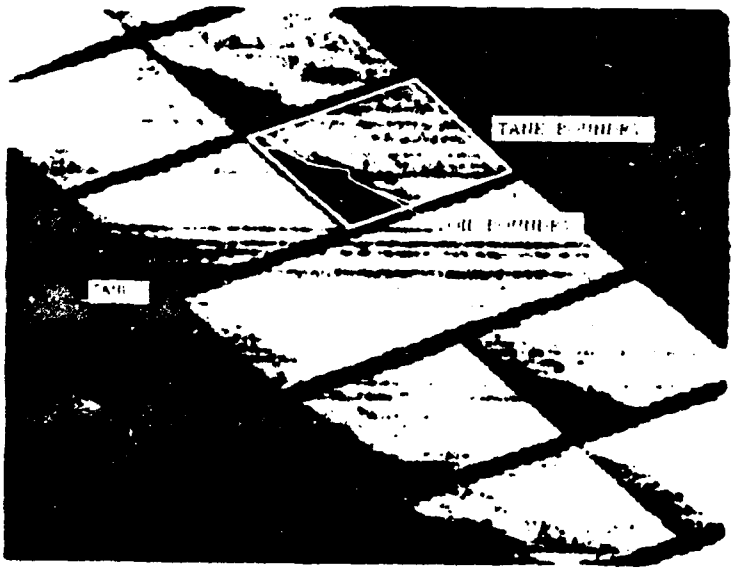

Figure 3-8. Example of Measuring Oil Slick and Tank Boundaries

Table 3-1. Oil Thickness Estimates in Millimeters from 5 May Image and Surface Truth Data

MEASUREMENT SOURCE	TANK NUMBER																	
	1N	1S	2N	2S	3N	3S	4	5N	5S	6N	6S	7N	7S	8	9N	9S	10N	10S
DAY																		
Environment Canada Area Measurement*	2.1	1.4	1.2	2.0	3.0	1.9	N/A	3.0	1.7	3.8	3.2	4.4	4.4	N/A	3.2	3.9	3.2	5.2
IRC-160ST		1.3	4.8	5.9	4.2	3.4	N/A	2.6	5.5	5.0	5.8	5.3	5.4	N/A	4.0	5.2	4.0	
FLIR 2000			5.0	5.1	3.6		N/A					6.2	6.8	N/A	5.2		4.3	
WF-360TL	2.7	3.0	2.0	2.1	2.2	2.6	N/A	2.6	3.5	6.1	5.3	3.9	3.8	N/A	4.0	4.8	6.3	6.3
WF-360TL (TV)	2.5	3.0	2.6	2.5	1.8	1.9	N/A	2.7	3.1	5.5		4.4	4.5	N/A	3.7	4.0	6.8	6.2
NIGHT																		
IRC-160ST	8.3	10.8	6.0	8.1	10.5	12.9	N/A	19.2		15.4	14.4	13.5	10.9	N/A	12.2	19.7	14.3	
FLIR 2000	6.0	8.1	5.7	7.3	16.3	16.2	N/A				13.8		6.7	N/A	11.5			
WF-360TL	7.7		4.1	4.5	6.1	8.4	N/A		11.0	12.2	12.4	8.8	8.2	N/A	11.2	13.2	13.8	12.7

* Time of measurements not recorded.

CHAPTER 4
CONCLUSIONS AND RECOMMENDATIONS

4.1 CONCLUSIONS

The following conclusions are based on the qualitative image analyses and sensor operator comments provided in chapter 2 and the more detailed image analyses conducted in chapter 3.

4.1.1 Infrared Imaging Performance

Daytime Oil/Water Contrast

Every IR sensor evaluated was capable of providing at least a minimal ability to detect oil slicks on the water surface during the daytime sorties. The following qualifying statements apply:

1. In close-up viewing, the IRC-160ST, FSI Prism, FSI 2000, and WF-360TL all provided an ability to distinguish multiple grey shades as oil slick thickness varied. The AGEMA 210 provided good oil/water contrast, but with less grey-scale detail due to its lower spatial acuity.

2. In clear sunny weather, specular reflection can interfere with the MWIR sensors' ability to view scene details.

Nighttime Oil/Water Contrast

At night, there is marginal oil/water contrast available in the MWIR spectral band, and the ability of these sensors to depict an oil/water boundary is highly dependent on minor variations in environmental conditions and sensor tuning. Both LWIR FLIRs are able to reliably image oil slicks on water at night because of the superior oil/water contrast present in the LWIR band when both liquids are at the same physical temperature.

MWIR and LWIR Image Acuity

Where sufficient IR contrast exists between oil and water, the IRC-160ST and FLIR PRISM MWIR imagers and both LWIR FLIRs provide good spatial resolution and image quality for oil slick identification and tracking.

Visible Spectrum Reference Images

The availability of visible spectrum video for the WF-360TL proved to be an excellent aid in determining ground truth/validity of the IR images.

Although not included in the evaluation by design, the Dark Invader Owl NVG camera was able to readily depict oil slick locations because of their excellent contrast with the bright bottom reflections from the shallow test tank.

4.1.2 Influence of Operational Parameters

Incidence Angle

The IR imagers are capable of effective oil slick surveillance over a wide range of incidence angles. In marginal contrast situations, changing the incidence angle may improve oil slick visibility.

Video Polarity

Both the white = hot and the black = hot video polarity provided similar contrast, clear image detail, and equivalent resolution. Selection of video polarity is a matter of operator preference for display appearance.

Altitude/Field of View

As expected, altitude significantly affects image content and quality. A lower altitude provides greater scene detail; however, it also limits the field of view. While this is true for both fixed lens and switchable lens sensors, the ability to switch from a wide field of view to a narrow field of view permits easier classification of contrast features than does a fixed lens sensor.

The large size of the RS-18C FOV did not permit a fair evaluation of its ability to detect and map oil signatures in a test area as small as the Petawawa site.

4.1.3 Ergonomics/Human Factors

Hand-held Sensor Design

The man-machine interfaces of the fully-integrated FLIR 2000 and WF-360TL FLIRs were easier to operate than those of the hand-held imagers. With the exception of overly-sensitive tuning adjustment controls; however, the unwieldy nature of hand-held sensor operations did not diminish the ability to effectively image the oil slicks.

4.2 RECOMMENDATIONS

The following recommendations are offered concerning the employment, use, and further evaluation of remote sensors in the Coast Guard MEP mission. These recommendations are based primarily on the qualitative analyses provided in this report.

1. Operational guidance should be developed for using available IR devices in typical MEP mission areas such as:

- oil or chemical spill quick response,
- MARPOL, and
- marine inspections.

This should be achieved by obtaining IR oil slick images at night, under a broad range of representative operating conditions, with a variety of oil types.

2. When both LWIR and MWIR sensors are available for night oil spill surveillance, LWIR is preferred if a worst-case scenario of oil and water at equal temperature can be expected.

3. The superior nighttime oil/water contrast observed in the LWIR spectral band and the desire for a portable IR sensor indicates that an evaluation of hand-held LWIR sensors should be conducted.

4. When conducting area surveillance of oil slicks, IR sensors should be used in wide field of view at altitudes of 1000 to 1500 feet. Examination of slick edge detail should be done at lower altitudes when using fixed-lens IR sensors or in narrow field of view where available.

5. Simplifying cabling, consolidating components, and providing an automated coarse contrast/tune function to quickly adjust for ambient conditions could reduce the level of distraction to the operator while improving safety and mission effectiveness. Environmental response personnel who are trained to use hand-held sensors during operational missions should be properly fitted with a personal helmet and familiarized with aircraft communications gear and procedures.

6. More detailed analysis should be conducted on the ability of night vision cameras to detect oil slicks in the marine environment. Particular areas of interest include:

- the level of ambient lighting required to detect a slick;
- the ability of aircraft-mounted illuminators to expand the window of NVG use, and
- the ability of this type sensor to provide slick edge details and areal extent.

7. If the effort recommended above is successful, the complementary nature of the daytime WF-360TL IR and television camera images indicates that the addition of a night vision camera capability to FLIR-equipped aircraft may, prove to be a valuable aid to nighttime oil slick surveillance.

REFERENCES

1 Campana, S., Passive Electro Optical Systems (Infrared & Electro-Optical Systems Handbook, Vol. 5), Infrared Information Analysis Center, ERIM and SPIE Optical Engineering Press. 1993.

2. Horvath, R., Morgan, W.L., and Stewart, S.R., Optical Remote Sensing of Oil Slicks: Signature Analysis and Systems Evaluation, (Final Report), Willow Run Laboratories, University of Michigan, and U.S. Coast Guard (DAT), October 1971.

3. Hover, G.L. and Daniels, G.M., The Detection of Oil Spills at Night with Airborne Infrared Imaging Sensors, (in publication), U.S. Coast Guard R&D Center and MIT-Lincoln Laboratory, March 1994.